

1 **Late Weichselian and Holocene paleoceanography of Storfjordrenna, southern Svalbard**

2  
3 M. Łącka\*, M. Zajaczkowski\*, M. Forwick\*\*, W. Szczuciński\*\*\*

4  
5 \*Institute of Oceanology, Polish Academy of Sciences, Powstańców Warszawy 55, 81-712  
6 Sopot, Poland.

7 \*\*Department of Geology, University of Tromsø – The Arctic University of Norway, N-9037  
8 Tromsø, Norway

9 \*\*\*Institute of Geology, Adam Mickiewicz University in Poznan, Maków Polnych 16, 61-  
10 606 Poznań, Poland

11  
12 Correspondence address: Magdalena Łącka, Institute of Oceanology, Polish Academy of  
13 Sciences, Powstańców Warszawy 55, 81-712 Sopot, Poland, e-mail: [mlacka@iopan.gda.pl](mailto:mlacka@iopan.gda.pl)

35           **Abstract**

36

37           Multiproxy analyses (including benthic and planktonic foraminifera,  $\delta^{18}\text{O}$  and  $\delta^{13}\text{C}$

38 records, grain-size distribution, ice-rafted debris, XRF geochemistry and magnetic

39 susceptibility) were performed on a  $^{14}\text{C}$ -dated marine sediment core from Storfjordrenna,

40 located off of southern Svalbard. The sediments in the core cover the termination of Bølling-

41 Allerød, the Younger Dryas and the Holocene and reflect general changes in the

42 oceanography/climate of the European Arctic after the last glaciation. Grounded ice of the last

43 Svalbard-Barents Sea Ice Sheet retreated from the coring site c. 13,950 cal yr BP. During the

44 transition from the sub-glacial to glaciomarine setting, Arctic Waters dominated the

45 hydrography in Storfjordrenna. However, the waters were not uniformly cold and experienced

46 several warmer spells. A progressive warming and marked change in the nature of the

47 hydrology occurred during the early Holocene. Relatively warm and saline Atlantic Water

48 began to dominate the hydrography starting from approximately 9600 cal yr BP. Although the

49 climate in eastern Svalbard was milder at that time than at present (smaller glaciers), two

50 slight cooling periods were observed in 9000 - 8000 cal yr BP and 6000 - 5500 cal yr BP. A

51 change in the Storfjordrenna oceanography occurred at the beginning of the late Holocene

52 (i.e., 3600 cal yr BP) synchronously with glacier growth on land and enhanced bottom current

53 velocities. Although cooling was observed in the Surface Water, Atlantic Water remained

54 present in the deeper portion of the water column of Storfjordrenna.

55

56

57

58

59

60

61

62

63

## 64 **1 Introduction**

65

66 The northward flowing North Atlantic Current (NAC) is the most important source of heat  
67 and salt in the Arctic Ocean (Gammelsrod and Rudels, 1983; Aagaard et al., 1987; Schauer et  
68 al., 2004; Fig. 1b). The main stream of Atlantic Water (AW) flowing north to Fram Strait in  
69 the form of the West Spitsbergen Current (WSC) causes a dramatic reduction of the sea ice  
70 extent and thickness via the warming of the intermediate water layer in this region of the  
71 Arctic Ocean (Quadfasel et al., 1991; Serreze et al., 2003). Paleoceanographic (e.g.,  
72 Spielhagen et al., 2011; Dylmer et al., 2013) and instrumental (Walczowski and Piechura  
73 2006, 2007; Walczowski et al., 2012) investigations provide evidence of a recent  
74 intensification of the flow of AW in the Nordic Seas and the Fram Strait.

75 The Svalbard archipelago is influenced by two water masses: AW flowing northward from  
76 the North Atlantic and Arctic Water (ArW) flowing southwest from the northern Barents Sea  
77 (Fig. 1b). An oceanic front arising at the contact of different bodies of water is an excellent  
78 area for research of contemporary and past environmental changes. Intensification of AW  
79 flow and associated climate warming result in decreased sea-ice cover in the Svalbard fjords  
80 during winter (Berge et al., 2006) and an increased sediment accumulation rate (Zajączkowski  
81 et al., 2004; Szczuciński et al., 2009) and influence the pelage-benthic carbon cycling  
82 (Zajączkowski et al., 2010).

83 Paleoceanographic records indicate that AW was present along the western margin of  
84 Svalbard, at least during the last 12,000 years (e.g., Ślubowska et al., 2007; Werner et al.,  
85 2011; Rasmussen et al., 2013), and occasionally reached the Hinlopen Trough and Kvitøya  
86 Trough, thus transporting warmer and more saline water to the eastern portion of Svalbard  
87 from the north (Ślubowska-Woldengen et al., 2007; Ślubowska et al., 2008; Kubischta et al.,  
88 2010; Klitgaard Kristensen et al., 2013). Periods of enhanced inflow of AW during the  
89 Holocene led to the expansion of marine species that are absent or only rarely occurring at  
90 present. These species include the mollusc *Mytilus edulis* whose fossil remains are widely  
91 distributed in raised beach deposits on the western and northern coasts of Svalbard (e.g.,  
92 Feyling-Hanssen and Jørstad, 1950; Hjort et al., 1992). *Mytilus edulis* spawn at temperatures  
93 above 8°C to 10°C (Thorarinsdóttir and Gunnarson, 2003) and thus are considered to indicate  
94 higher surface-water temperature related to stronger AW inflow during the early Holocene  
95 (11,000 – 6800 cal yr BP) (Feyling-Hanssen, 1955; Salvigsen et al., 1992; Hansen et al.,  
96 2011). Although the progressive development of *Mytilus edulis* is well documented by  
97 periods of warming and inflow of AW to the Hinlopen Trough, the presence of this species in

98 Storfjorden (W Edgeøya; Fig. 1) is unclear. Hansen et al. (2011) suggested that a small branch  
99 of warm AW could have reached eastern Spitsbergen from the south at that time.

100 In the 1980s and 1990s, Storfjorden was thought to be exclusively influenced by the East  
101 Spitsbergen Current (ESC), which carries cold and less saline ArW from the Barents Sea  
102 (Quadfasel et al., 1988; Piechura et al., 1996). More recent studies suggested that the  
103 hydrography in Storfjorden is affected by the production of brine-enriched shelf waters (e.g.,  
104 Haarpaintner et al., 2001; Rasmussen and Thomsen, 2009), the creation of a coastal polynya  
105 (e.g., Skogseth et al., 2005; Geyer et al., 2010) or the overflow of dense waters to the  
106 continental shelf (e.g., Fer et al., 2003). However, hydrological data obtained from  
107 conductivity-temperature sensors attached to a *Delphinapterus leucas* showed a substantial  
108 and topographically steered inflow of AW to Storfjorden through the Storfjordrenna  
109 (Lydersen et al., 2002). Recently, Akimova et al. (2011) reviewed typical water masses for  
110 Storfjorden, where the AW was located between 50 and 70 meters.

111 Storfjordrenna is a sensitive boundary area (Fig. 1) where two contrasting water masses  
112 form an oceanic polar front separating the colder, less saline and isotopically lighter ArW  
113 from warmer, highly saline and  $\delta^{18}\text{O}$ -heavier AW. An abrupt cooling (e.g., Younger Dryas,  
114 Little Ice Age) and warming (e.g., early Holocene warming) of the European Arctic might be  
115 linked to relatively small displacements of this front (Sarnthein et al., 2003; Hald et al., 2004;  
116 Rasmussen et al., 2014).

117 Two sediment cores collected at the mouth of Storfjordrenna reveal a continuous inflow of  
118 AW to the southwestern Svalbard shelf since the deglaciation of Svalbard-Barents Ice Sheet  
119 (Rasmussen et al., 2007), whereas the inner Storfjorden basins underwent a shift from  
120 occupation by continental ice to an ice proximal condition (Rasmussen and Thomsen, 2014).  
121 Nevertheless, a limited amount of paleoceanographical data are available from this region,  
122 and thus the reconstruction of the Svalbard-Barents Ice Sheet retreat and the further  
123 development of Storfjordrenna oceanography are often speculative.

124 In this paper, we present results from multi-proxy analyses of a sediment core retrieved  
125 100 km east of the mouth of Storfjordrenna (Fig. 1a). We provide a new age for the retreat of  
126 the last Svalbard-Barents Sea Ice Sheet from Storfjordrenna and discuss the interaction of  
127 oceanography and deglaciation as well as the postglacial history of Atlantic Water inflow  
128 onto the shelf off of southern Svalbard. Because the studied sediment core was retrieved from  
129 an oceanographic frontal zone, which is sensitive to larger-scale changes, we believe that the  
130 presented data show the general climatic/oceanographic trends in the eastern Arctic.

131

## 132 **2 Oceanographic setting**

133

134 Storfjorden is an approximately 190-km long and up to 190-m deep glacial trough located  
135 between the landmasses of Spitsbergen to the west, Edgeøya and Barentsøya to the east, and  
136 the shallow Storfjordenbanken to the southeast (Fig. 1a). It is not a fjord *sensu stricto* because  
137 the sounds of Heleysundet and Freemansundet to the north and northeast, respectively,  
138 connect the head of Storfjorden to the northwestern Barents Sea. A sill of 120-m depth  
139 crosses the mouth of Storfjorden. The 254-km long Storfjordrenna, a continuation of the  
140 trough that extends towards the shelf break, is located beyond this sill. The bottom depth  
141 along the trough axis varies between 150 m and 420 m (Pedrosa et al., 2011).

142 The water column of Storfjorden and Storfjordrenna is composed of two main water  
143 masses transported with currents from the east and south and mixed waters that are formed  
144 locally (Table 1. after Skogseth et al., 2005). Warm and saline Atlantic Water (AW) enters  
145 Storfjordrenna in a cyclonic manner (Schauer, 1995; Fer et al., 2003), flowing into the trough  
146 parallel to its southern margin and flowing towards the trough mouth along its northern slope.  
147 The AW occurs between 50 m and 70 m in Storfjorden and extends to a depth of 200 m in  
148 Storfjordrenna (Akimova et al., 2011). The origin of AW entering Storfjordrenna is an  
149 eastward branch of the North Atlantic Current (NAC) following the topography of the Barents  
150 Sea Shelf Break. However, approximately 50% of the AW flowing northward also penetrates  
151 into Bjørnøyrenna (Smedsrud et al., 2013; for location, see Fig. 1). The AW in Storfjordrenna  
152 is cooler and fresher than in Bjørnøyrenna as an effect of the distance and mixing processes  
153 (O'Dwyer et al., 2001). The AW may occasionally propagate even further east of Svalbard,  
154 where it fills depressions below 180 m (Schauer, 1995). Relatively cold Arctic Water (ArW)  
155 is transported to Storfjorden and Storfjordrenna by the East Spitsbergen Current (ESC). The  
156 ESC enters the fjord through the tidally influenced sounds of Heleysundet and Freemansundet  
157 in the north and northeast (Norges Sjøkartverk, 1988) as well as from the southeast with a  
158 coastal current flowing near Edgøya (Loeng, 1991). The AW and ArW mix to form  
159 Transformed Atlantic Water (TAW), which dominates on the shelf off of west Spitsbergen  
160 (Svendsen et al., 2002; Table 1). Dense, brine-enriched Shelf Water (BSW) in Storfjorden is  
161 produced through high polynya activity and results from intense formation of sea ice  
162 (Haarpaintner et al., 2001; Skogseth et al., 2004, 2005). The BSW fills the fjord to the top of  
163 the sill (120 m) and initiates a gravity-driven overflow (Quadfasel et al., 1988; Schauer, 1995;  
164 Schauer and Fahrbach, 1999; Fer et al., 2003, 2004; Skogseth et al., 2005). The BSW is  
165 characterised by a salinity value greater than 34.8 and a temperature at or slightly above the

166 freezing point (Table 1). Surface Water (SW) in the upper 50 m is cold and fresh during the  
167 autumn and warm and fresh during the summer due to ice melting. In winter, the water  
168 column in Storfjorden is homogenised due to wind and tidal mixing and is considered to have  
169 a temperature close to the freezing point (Skogseth et al., 2005).

### 170 **3 Materials and methods**

171

172 Multi-proxy analyses of the gravity core JM09-020-GC provided the foundation for this  
173 study. The core was retrieved with R/V Jan Mayen (University of Tromsø – The Arctic  
174 University of Norway, UiT) in November 2009 from the Storfjordrenna (76°31489' N,  
175 19°69957' E) at a bottom depth of 253 m (Fig. 1a). The coring site was located in an area  
176 above the continuous presence of BSW and was selected after an echo-acoustic investigation  
177 to identify the greatest possible area of flat bottom with a minimum disturbance of sediments.  
178 Conductivity-temperature-depth (CTD) measurements were performed prior to coring (Fig.  
179 2a) and in summer 2013 (Fig. 2b).

180 Prior to sediment core opening, the magnetic susceptibility (MS) was measured using a  
181 loop sensor installed on a GEOTEK Multi Sensor Core Logger at the Department of Geology,  
182 UiT. Core sections were stored in the laboratory for one day prior to measurements, thus  
183 allowing the sediments to adjust to room temperature and avoiding measurement errors  
184 related to temperature changes (Weber et al., 1997). The X-radiographs and digital images  
185 were collected from half of the core to define the sedimentary and biogenic structures. The  
186 sediment colour was defined according to the Munsell Soil Color Charts (Munsell Products,  
187 2009). Qualitative element-geochemical measurements were performed with an Avaatech X-  
188 ray fluorescence (XRF) core scanner using the following settings: 10 kV, 1000  $\mu$ A, 10-s  
189 measuring time, and no filter. Both core halves were subsequently cut into 1-cm slices and  
190 transported to the Institute of Oceanology at the Polish Academy of Sciences in Sopot for  
191 further analyses.

192 Sediment samples for foraminiferal analyses were freeze-dried, weighed, and wet sieved  
193 using sieves with mesh sizes of 500  $\mu$ m and 100  $\mu$ m. The residues were dried, weighed again  
194 and subsequently split on a dry micro-splitter. Where possible, at least 300 specimens of  
195 foraminifera were counted in every 5 cm of sediment. Species identification under a binocular  
196 microscope (Nikon SMZ1500) was supported using the classification of Loeblich and Tappan  
197 (1987), with few exceptions, and percentages of the eight indicator species were applied. The  
198 number of species per sample and Shannon-Wiener Index were calculated using the program

199 Primer 6. The benthic foraminiferal abundance and ice-rafted debris (IRD; grains >500  $\mu\text{m}$ )  
200 were counted under a stereo-microscope and expressed as flux values (number of  
201 specimens/grains  $\text{cm}^{-2} \text{ka}^{-1}$ ) using the bulk sediment density and sediment accumulation rate.

202 Stable oxygen and carbon isotope compositions of tests of the infaunal foraminifer species  
203 *Elphidium excavatum* f. *clavata* were determined at the Department of Geological Sciences,  
204 University of Florida (Florida, USA). All values are calibrated to the PeeDee Belemnite  
205 (PDB) scale and corrected for ice volume changes. In our study, we discuss the  $\delta^{18}\text{O}$  and  $\delta^{13}\text{C}$   
206 record as a relative measure for changes in the water mass characteristics (temperature-  
207 salinity) and/or the supply of meltwater/freshwater to the area. Moreover, no reliable vital  
208 effect correction has been created for *E. excavatum* f. *clavata* (Bauch et al., 2004; Ślubowska-  
209 Woldengen et al., 2007), and therefore, we did not correct the isotopic values for vital effect.

210 Grain size (<2 mm) analyses were performed every 1 cm using a Malvern Mastersizer  
211 2000 laser particle analyser and presented as volume percent. To examine the relative  
212 variability in the near-bottom currents, the mean grain-size distribution of the <63- $\mu\text{m}$  fraction  
213 was calculated to avoid the effect of ice-rafted coarse fraction. The mean grain size was  
214 calculated using the program GRADISTAT 8.0 according to the geometric method of  
215 moments (Blott and Pye, 2001).

216 The chronology for this study is based on high-precision AMS  $^{14}\text{C}$  measurements of  
217 fragments from nine calcareous bivalve shells. Measurements were performed in the Poznań  
218 Radiocarbon Laboratory, which is equipped with a 1.5 SDH-Pelletron Model "Compact  
219 Carbon AMS" (Czernik and Goslar, 2001; Goslar et al., 2004). The surface layer of shells was  
220 scraped off to avoid contamination with younger carbonate encrustation. The AMS  $^{14}\text{C}$  dates  
221 were converted into calibrated ages using the calibration program CALIB 6.1 (Stuiver and  
222 Reimer, 1993; Stuiver et al., 2005) and the Marine13 calibration curve (Reimer et al., 2013).  
223 The difference  $\Delta R$  in reservoir age correction of the model ocean and region of Svalbard was  
224 reported by Mangerud et al. (2006) as  $105 \pm 24$  or  $111 \pm 35$ , and we used the first value. The  
225 calibrated ages are presented in Table 2. It should be noted that the reservoir age is based on a  
226 few data points from western Spitsbergen, and the age may be different for the eastern coast.  
227 However, no data are available from the latter region.

228

## 229 **4 Results**

230

### 231 **4.1 Modern hydrology**

232

233 In November 2009, the Surface Water at the coring site (upper ~27 m) had already cooled  
234 (1.24°C; Fig. 2a); however, its salinity was still low (34.24). Transformed AW was observed  
235 in the layer between 60 m and 160 m. The lowermost portion of the water column shows  
236 evidence of gradual cooling that reached a minimum temperature of 0.76°C near the bottom.  
237 The lack of BSW at the bottom indicates gradual water mixing during summer and fall. In  
238 August 2013, the Surface Waters had a slightly lower salinity, but the temperature was ~5°C  
239 higher than in November 2009 (Fig. 2b). The TAW occupied the same depths as in 2009.  
240 However, an almost 50-m thick layer of BSW was present close to the seafloor.

241

## 242 **4.2 Age model**

243

244 The <sup>14</sup>C ages and calibrated ages are reported in Table 2. The calibration gives an age  
245 distribution and not a single value; thus, the 2-sigma range is presented, and Fig. 3 shows the  
246 age probability distribution curves. The ages of the samples generally increase with sediment  
247 depth except in the case of one sample, i.e., St 20A 39, which provided an older age than the  
248 sample below. That shell was most likely re-deposited and thus was not used for the age  
249 model. However, because all of the samples used for dating were shell fragments, it must be  
250 noted that it is possible that more samples could be subjected to re-deposition, but based on  
251 the available data, it is not possible to confirm. The age model is based on the assumption of  
252 linear sediment accumulation rates between data points. The highest probability peaks from  
253 the calibrated age ranges were used as input values for the model. For the lowermost and  
254 uppermost regions of the core, we adopted sediment accumulation rates for the neighbouring  
255 region. It is common to observe the loss of the sediment surface layer during coring with  
256 heavy gravity cores. In the case of core JM09-020-GC, it is likely that at least the top 40 cm  
257 of sediments were lost during coring. This conclusion is supported by analysis of a box corer  
258 collected prior to coring (Łącka et al., in prep.). The extrapolated age model for the sediment  
259 surface is therefore 1200 cal yr BP.

260

## 261 **4.3 Sedimentological and geochemical parameters**

262

263 The core JM09-020-GC is 426 cm long and consists of four lithological units: L1  
264 (bottom of the core to 370 cm; >13,450 cal yr BP), L2 (370 cm to 272 cm; ~13,450 cal yr BP  
265 to ~11,500 cal yr BP), L3 (272 cm to 113 cm; ~11,500 cal yr BP to ~3600 cal yr BP) and L4  
266 (113 cm to core top; ~3600 cal yr BP to ~ 1200 cal yr BP). The lithological log was created



267 based on the X-radiographs, grain-size analysis data and foraminiferal flux (Fig. 4). Grains >2  
268 mm are referred to as “clasts” and are marked in the lithological logs as individual features.

269 Unit L1 consists of compacted massive dark grey (5Y 4/1) sandy mud with various  
270 amounts of clasts. Bioturbation and foraminifera were generally absent. However, one shell  
271 fragment was found at approximately 395 cm.

272 Unit L2 contains massive dark grey (5Y 4/1) sandy mud with an amount of coarser  
273 material and generally lower amounts of clasts than unit L1. The mean grain size (<63  $\mu\text{m}$ )  
274 ranged from 7-10  $\mu\text{m}$ . The highest IRD flux and Fe/Ca ratio for the entire core occur in this  
275 unit. The mass accumulation rate (MAR) is 0.043  $\text{g cm}^{-2} \text{yr}^{-1}$ . The first signs of bioturbation  
276 occur in this unit, and the flux of foraminifera increases rapidly up to ~5700 individuals  $\text{cm}^{-2}$   
277  $\text{ka}^{-1}$  (Fig. 4).

278 The unit L3 is composed of massive dark olive grey mud (5Y 3/2) and is characterised  
279 by decreasing MAR values (0.019  $\text{g cm}^{-2} \text{yr}^{-1}$  to 0.002  $\text{g cm}^{-2} \text{yr}^{-1}$ ), moderate sand content and  
280 clearly increasing mean grain size (<63  $\mu\text{m}$ ). The IRD flux is low, and the Fe/Ca ratio  
281 decreases gradually until c. 9200 cal yr BP and remains low (between 3 and 4; Fig. 4)  
282 Continuous bioturbation and variable foraminiferal fluxes are observed, with maxima in the  
283 intervals 9000-8000 cal yr BP and 6000-5500 cal yr BP.

284 The uppermost unit L4 is primarily composed of the same material as the underlying  
285 unit, i.e., massive dark olive grey mud (5Y 3/2). However, the sand content is occasionally  
286 higher. The MAR increases to 0.024  $\text{g cm}^{-2} \text{yr}^{-1}$ . The mean grain size (<63  $\mu\text{m}$ ) throughout  
287 this interval is even higher than that in L3 and reaches up to 15  $\mu\text{m}$ ; the Fe/Ca ratio is  
288 increasing. The bioturbation continues, numerous shell fragments are present, and the  
289 foraminifera flux reaches high values throughout the entire unit.

#### 290 **4.4 Foraminiferal fauna**

291  
292 A total of 54 calcareous and 6 agglutinated species were identified. The foraminiferal  
293 assemblages were dominated by calcareous fauna. Agglutinated species occurred only in 14  
294 sediment samples, and their abundance did not exceed 4%. The only exception is the sample  
295 dated to c. 11,350 cal yr BP (262.5 cm depth) with 25% of agglutinated foraminiferal fauna.  
296 However, in this sample, the total foraminifera abundance was low (13 specimens  $\text{g}^{-1}$   
297 sediment). In general, species richness, number of agglutinated foraminifera, and rare and  
298 fragile species increase towards the top of the core. Benthic foraminiferal fauna is dominated  
299 by *Elphidium excavatum* f. *clavata*, *Cassidulina reniforme*, *Nonionellina labradorica*,

300 *Melonis barleeaanum*, *Islandiella* spp. (*Islandiella norcrossi*/*Islandiella helenae*) and *Cibicides*  
301 *lobatulus*. Percentages of *E. excavatum* f. *clavata* show an inverse relationship to *C.*  
302 *reniforme* with the almost constant dominance of the latter species in the periods ~12,450 cal  
303 yr BP to ~12,000 cal yr BP and ~9600 cal yr BP to ~2800 cal yr BP (Fig. 5). Planktonic  
304 foraminifera are represented by three species, i.e., *Neogloboquadrina pachyderma* (sinistral),  
305 *Neogloboquadrina pachyderma* (dextral) and *Turborotalita quinqueloba*. However, the two  
306 latter species are quite rare. In general, the abundance of planktonic fauna is low in the older  
307 portions of the core and slightly increases at approximately 10,000 cal yr BP, reaching  
308 maximum values c. 2000 cal yr BP (Fig. 5).

309 Based on the most significant changes in the foraminiferal species abundances, species  
310 diversity, and  $\delta^{18}\text{O}$  and  $\delta^{13}\text{C}$  in *E. excavatum* f. *clavata* tests, the core was divided into four  
311 foraminiferal zones F1-F4: ~13,450 cal yr BP to 11,500 cal yr BP (F1); 11,500 cal yr BP to  
312 9200 cal yr BP (F2); 9200 cal yr BP to 3600 cal yr BP (F3); and 3600 cal yr BP to 1200 cal yr  
313 BP (F4) (Fig. 5). The zones correspond to lithological divisions. The age of unit F4 is the  
314 same as L4, units F3 and F2 correspond to L3, and unit F1 is linked to unit L2. In unit L4,  
315 foraminifera are rare to absent.

316 Zone F1 is dominated by the opportunistic *E. excavatum* f. *clavata* and *C. reniforme*.  
317 The latter species dominates over *E. excavatum* f. *clavata* between 12,250 cal yr BP and  
318 11,950 cal yr BP. High percentages of *C. lobatulus* (up to 57%) and *Astrononion gallowayi*  
319 (up to 2.5%) occur occasionally. The planktonic foraminifera flux was low at the beginning of  
320 this section (mean value of 9 specimens  $\text{cm}^{-2} \text{ka}^{-1}$ ) and completely disappeared for nearly  
321 1500 years from approximately 11,500 cal yr BP (Fig. 5). The species richness and the  
322 Shannon-Wiener index show low biodiversity compared with the upper portion of the core  
323 (mean values of 8 and 1.26, respectively). Furthermore, maxima of  $\delta^{18}\text{O}$  and  $\delta^{13}\text{C}$  occur in  
324 this interval.

325 In zone F2, the contribution of *E. excavatum* f. *clavata* and *C. reniforme* is slightly  
326 lower, and *N. labradorica* becomes the most abundant species (Fig. 5). There is also an  
327 increase in *Islandiella* spp. percentage. Planktonic foraminifera appeared again c. 10,000 cal  
328 yr BP. Biodiversity significantly increased, and  $\delta^{18}\text{O}$  reached its minimum value of 2.61‰ vs.  
329 VPDB at approximately 10,000 cal yr BP.

330 Zone F3 is characterised by the minimum mass accumulation rates of sediment and  
331 consequent low temporal resolution. *C. reniforme* dominates over *E. excavatum* f. *clavata*  
332 throughout. *M. barleeaanum* has its maximum abundance in this zone, and *N. labradorica* is  
333 abundant in the lower portions of this zone, decreasing at approximately 7000 cal yr BP.

334 *Islandiella* spp. increases upcore. Planktonic foraminifera occur in the entire zone, and the  
335 fluxes are higher than those of previous units (Fig. 5). Biodiversity remains high in this zone,  
336 and  $\delta^{18}\text{O}$  and  $\delta^{13}\text{C}$  remain generally stable; however, marked peaks occurred at approximately  
337 6800 cal yr BP, 6500 cal yr BP and 5700 cal yr BP, respectively.

338 A consistently high foraminiferal flux of up to  $\sim 4900$  specimens  $\text{cm}^{-2} \text{ka}^{-1}$   
339 characterises zone F4. The fluxes of *Islandiella* spp. and *Buccella* spp. increase significantly,  
340 and from 2850 cal yr BP, *Islandiella* spp. dominated the assemblage with *E. excavatum*  
341 *f. clavata*. Additionally, the fluxes of *C. lobatulus* and *A. gallowayi* increase; however, their  
342 abundances are lower than those of zone F2. A maximum abundance of planktonic  
343 foraminifera occurs in this unit. Foraminifera biodiversity continues to increase towards the  
344 core top (up to 2.33; Fig. 5), and  $\delta^{18}\text{O}$  and  $\delta^{13}\text{C}$  increase slightly with numerous fluctuations.

345

## 346 **5 Discussion**

347 The European Arctic includes continental slope strongly influenced by north flowing  
348 Atlantic water and large shelf of the Barents Sea characterised by less saline and colder water.  
349 The available broad range of studies concerning paleoceanography of the European Arctic  
350 focus on its marginal sites: westernmost (e.g. Rasmussen et al., 2007; Eldevik et al., 2014;  
351 Sternal et al., 2014), northern (Wollenburg et al., 2004, Klitgaard Kristensen et al., 2014) and  
352 eastern (Polyak and Solheim, 1994), while the border zone lying between the slope of  
353 continental shelf and central Barents Sea is poorly studied. The lack of well-defined and  
354 sufficiently complete paleoceanographic record containing the signal from both of these  
355 environments has encouraged the authors to study a sediment core retrieved inside  
356 Storfjordrenna, especially in the light of current hydrological changes in this area (e.g.  
357 Lydersen et al., 2002; Skogseth et al., 2005; Akimova et al., 2011). This location should  
358 present the general trends in the eastern Arctic, including Svalbard glacier activities, pack-ice  
359 in the Arctic Ocean and North Atlantic water circulation, moreover it avoids the local (fjordic)  
360 condition. We have decided to discuss the presented record chronologically as a postglacial  
361 interplay between two hydrological regimes. Based on the most pronounced changes in  
362 sedimentological and foraminiferal data as well as comparisons with previous studies from  
363 adjacent areas, we distinguish five units in the studied core: a sub-glacial unit ( $>13,450$  cal yr  
364 BP), a glacier-proximal unit (13,450 cal yr BP to 11,500 cal yr BP), a glaciomarine unit I  
365 (11,500 cal yr BP to 9200 cal yr BP), a glaciomarine unit II (9200 cal yr BP to 3600 cal yr  
366 BP) and a glaciomarine unit III (3600 cal yr BP to 1200 cal yr BP).

## 367 **5.1 Sub-glacial unit (>13,450 cal yr BP)**

368 The lowermost unit L1 (Fig. 4) was significantly coarser, more compacted and devoid  
369 of foraminifera, which indicates that it is likely of sub-glacial origin. During the late  
370 Weichselian Glacial Maximum, Storfjorden and Storfjordrenna were covered by an ice stream  
371 that drained the Svalbard-Barents Ice Sheet (SBIS; e.g., Ottesen et al., 2005). The SBIS  
372 deglaciation occurred as a response to the sea-level rise and increased mean annual  
373 temperature (Siegert and Dowdeswell, 2002). Rasmussen et al. (2007) noted that the outer  
374 portion of Storfjordrenna (389-m depth; Fig. 1a) was deglaciated prior to 19,700 cal yr BP.  
375 The bivalve shell fragment from 395.5 cm in our core suggests that the centre portion of  
376 Storfjordrenna was ice-free before ~13,950 cal yr BP. This observation indicates that the  
377 ~100-km long retreat of the grounding line from the shelf break to the central portion of  
378 Storfjordrenna occurred over approximately 5700 years. The deglaciation of the inner  
379 Storfjorden basin occurred c. 11,700 cal yr BP (Rasmussen and Thomsen, 2014), whereas the  
380 coasts of the east Storfjorden islands, Barentsøya and Edgeøya, which are located over 100  
381 km north from the coring site, occurred some 500 years later, i.e., 11,200 cal yr BP  
382 (recalibrated after Landvik et al., 1995). Siegert and Dowdeswell (2002) noted that during the  
383 Bølling-Allerød warming (c. 14,700-12,700 cal yr BP), certain of the deeper bathymetric  
384 troughs (e.g., Bjørnøyrenna) had deglaciated first, and large embayments of ice formed  
385 around them. It is likely that Storfjordrenna was one of such embayments at that time. Our  
386 data are in agreement with ice stream retreat dynamics presented by Rütther et al. (2012) and  
387 refine the recent models of the Barents Sea deglaciation (e.g., Winsborrow et al., 2010;  
388 Hormes et al., 2013; Andreassen et al., 2014).

## 389 **5.2 Glacier-proximal unit (13,450 cal yr BP to 11,500 cal yr BP)**

390  
391 The transition from a subglacial to glaciomarine setting is observed as a distinct change in  
392 sediment colour, several peaks of IRD, a decreased amount of clasts and the appearance of  
393 foraminifera. The sediment accumulation rate ( $0.043 \text{ g cm}^{-2} \text{ yr}^{-1}$ ) was of the same order of  
394 magnitude as that of the modern proximal and central regions of the west Spitsbergen fjords  
395 (see Szczuciński et al., 2009 for a review). Textural and compositional analyses of L2  
396 recorded a bimodal grain-size distribution and low abundance of microfossils, suggesting that  
397 deposition during the deglaciation occurred due to suspension settling from sediment-laden  
398 plumes and ice rafting (Lucchi et al., 2013; Witus et al., 2014). This unit in our core is limited  
399 to ~60 cm and is characterised by a lack of bioturbation in its lower portion.

400 The high flux of IRD is supported by the high Fe/Ca ratio and the depleted  $\delta^{18}\text{O}$  values  
401 correlate well with the abundance of *C. lobatulus* and *A. gallowayi* (Fig. 4 and Fig. 5), two  
402 species connected with high energy environments (Østby and Nagy, 1982), thus indicating  
403 that the coring site was likely located proximal to one or several ice fronts during the time of  
404 deposition of this unit.

405 During an early phase of the deglaciation of Storfjorden, the East Spitsbergen Current  
406 was still not active because the ice sheet grounded between Svalbardbanken and  
407 Storfjordbanken blocked the passage between eastern and western Svalbard (Rasmussen et  
408 al., 2007; Hormes et al., 2013). Thus, the first foraminiferal propagules (juvenile forms) were  
409 transported by sea currents (Alve and Goldstein, 2003) from the south and west and settled on  
410 the seafloor that was exposed after the retreat of grounded ice. The proximal glaciomarine  
411 environment affected the foraminiferal assemblages and resulted in low species richness,  
412 biodiversity and low foraminiferal abundance. Consequently, foraminifera assemblages  
413 became dominated by fauna typical of the glacier proximal settings: *E. excavatum* f. *clavata*,  
414 *C. reniforme* and *Islandiella* spp. (e.g., Vilks, 1981; Osterman and Nelson, 1989; Polyak and  
415 Mikhailov, 1996; Hald and Korsun, 1997). The dominance of *E. excavatum* f. *clavata*  
416 confirms the proximity to the ice sheet, decreased salinity and high water turbidity (e.g.,  
417 Steinsund, 1994; Korsun and Hald, 1998; Włodarska-Kowalczyk et al., 2013).

418 The upper portion of unit L2 (c. 12,800-11,500 cal yr BP) spans the Younger Dryas (YD)  
419 stadial. Records of marine sediments from Nordic and Barents Seas (e.g., Rasmussen et al.,  
420 2007; Ślubowska-Woldengen et al., 2007, 2008; Zamelczyk et al., 2012; Groot et al., 2014),  
421 as well as  $\delta^{18}\text{O}$  records from Greenland ice cores (e.g., Dansgaard et al., 1993; Grootes et al.,  
422 1993; Mayewski et al., 1993; Alley, 2000) show that the YD was characterised by a rapid and  
423 short-term temperature decrease. This event was likely driven by the weakened North Atlantic  
424 Meridional Overturning Circulation, a result of the Lake Agassiz outburst (e.g., Gildor and  
425 Tziperman, 2001; Jennings et al., 2006; Murton et al., 2010; Cronin et al., 2012) or the  
426 interaction between the sea ice and thermohaline water circulation (Broecker, 2006), which  
427 led to a reduction of AW transport to the north and a dominance of fresher Arctic Water. Our  
428 data show that the heavier  $\delta^{18}\text{O}$  values recorded, e.g., 12,720 cal yr BP and 12,100 cal yr BP,  
429 correlate with reduced to absent IRD fluxes, whereas the peaks of lighter  $\delta^{18}\text{O}$ , e.g., 12,450  
430 cal yr BP, 12,150 cal yr BP, and 11,780 cal yr BP, occurred synchronously with significant  
431 enhanced IRD fluxes (Fig. 6). The absence of IRD, occasionally for several decades, might  
432 reflect temporary polar conditions (Dowdeswell et al., 1998; Gilbert, 2000) characterised by  
433 the formation of perennial pack ice in Storfjorden that locked icebergs proximal to their

434 calving fronts and prevented their movement over the coring site (Forwick and Vorren, 2009).  
435 Wollenburg et al. (2004) observed a decrease in paleoproductivity on the northern Barents  
436 Sea margin between 12,800 cal yr BP and 12,500 cal yr BP and the later paleoproductivity  
437 peak at the termination of YD; they concluded that permanent sea ice cover causes the  
438 decrease in sea productivity, whereas enhanced advection of Atlantic Water to the site might  
439 result in paleoproductivity increase. Those periods of accelerated AW inflow resulted in  
440 massive iceberg rafting and delivery of IRD to Storfjordrenna, thus reflecting more sub-polar  
441 conditions. Hydrological variability during the Younger Dryas was previously noted in  
442 selected circum-North-Atlantic deep-water records (Bakke et al., 2009; Elmore and Wright,  
443 2011 and references therein; Pearce et al., 2013). Moreover, oxygen stable isotopes records  
444 from an ice-core GISP2 show certain warmer spells during that time (Stuiver et al., 1995),  
445 which coincides with higher ice rafting in Storfjordrenna (Fig. 6). Bakke et al. (2009) noted  
446 that the earlier portion of YD was colder and more stable, whereas the latter portion of this  
447 period was characterised by alternations between sea-ice cover and an influx of warmer and  
448 saltier North Atlantic waters. Our records show that during the late YD, the  $\delta^{18}\text{O}$  data were  
449 slightly shifted towards lighter values. Temporal resolution of our records does not allow for  
450 more detailed comparison with available data; nevertheless, they clearly indicate that the  
451 Younger Dryas was not uniformly cold and that at least a number of warmer spells occurred  
452 on eastern Svalbard.

453 We also conclude that the data on  $\delta^{18}\text{O}$  presented in Fig. 6 reflect temperature variations at  
454 the coring site according to the isotopically lighter ArW paleotemperature model (Duplessy et  
455 al., 2005). Another explanation for the heavier  $\delta^{18}\text{O}$  periods during the YD could be the  
456 intermittent inflow of warmer AW; however, this is unlikely to cause the synchronous  
457 disappearance of IRD.

458

### 459 **5.3 Glaciomarine unit I (early Holocene; 11,500 cal yr BP to 9200 cal yr BP)**

460

461 During the early Holocene, foraminiferal fauna, although low in abundance, were  
462 dominated by species related to the glaciomarine environment (*E. excavatum* and *C.*  
463 *reniforme*; Fig. 5). Increasing species richness and biodiversity of foraminifera point to  
464 amelioration of environmental conditions and a progressive increase in the distance to the  
465 glacier front (Korsun and Hald, 2000; Włodarska-Kowalczyk et al., 2013). The decrease of  
466 the Fe/Ca ratio is suggested to reflect increased the marine productivity and a reduced supply  
467 of terrigenous material (Croudace et al., 2006). The mean grain size ( $>63\ \mu\text{m}$ ; Fig. 4)

468 indicates weaker bottom currents at the beginning of the early Holocene and stronger bottom  
469 currents at the end of this period, which might be related to the ongoing isostatic uplift of the  
470 land masses of Svalbard as well as the sea level rise (e.g., Forman et al., 2004).

471 Significant fluctuations of  $\delta^{18}\text{O}$  and  $\delta^{13}\text{C}$  and increasing abundance of *N. labradorica*  
472 and *Islandiella* spp. suggest that Storfjordrenna was under the influence of various water  
473 masses at this time (Fig. 5). Comparison of our  $\delta^{18}\text{O}$  records with records from the  
474 Storfjorden shelf (400-m depth; Rasmussen et al., 2007; Fig. 1a) and the northern shelf of  
475 Svalbard (400-m depth; Ślubowska et al., 2005; Fig. 1b) shows that all of the records are  
476 shifted towards lighter values in the early Holocene (Fig. 7a), and the record from our core  
477 shows the most depletion (from c. 13,000 cal yr BP). We suggest that the records located on  
478 the western and northern shelf of Svalbard directly mirror the effect of warmer Atlantic Water  
479 inflow, whereas records from Storfjordrenna were under the influence of isotopically lighter  
480 Arctic Water from the Barents Sea (Duplessy et al., 2005). The shift from the Arctic Water  
481 domain to the Atlantic Water domain during the end of the early Holocene is also visible on a  
482 scatter plot of  $\delta^{13}\text{C}$  against  $\delta^{18}\text{O}$  (Fig. 7b). The results grouped to the left indicate Arctic  
483 Water domination, whereas the results grouped to the right show Atlantic Water domination.

484 According to Kaufman et al. (2004), the early Holocene is characterised by higher  
485 summer solar insolation at 60°N (10% higher than today), leading to a reduction in sea-ice  
486 cover (Sarnthein et al., 2003). As ice cover decreased, additional solar energy was stored in  
487 summer and subsequently re-radiated during the winter (e.g., Gildor and Tziperman, 2001).  
488 This process accelerated the ice sheet melting, and eventually, its retreat towards the fjord  
489 heads (Forwick & Vorren, 2009; Jessen et al., 2010; Baeten et al., 2010). Our data suggest  
490 that the iceberg calving to Storfjordrenna was significantly reduced or may have even  
491 disappeared at approximately 10,800 cal yr BP. However, the supply of turbid meltwater from  
492 land to the study area still resulted in a relatively high sediment accumulation rate.

493 According to Risebrobakken et al., (2011) and Groot et al., (2014), the presence of  
494 Arctic Water suppressed the warming signal in the western Barents Sea. This observation is in  
495 agreement with our data on planktonic foraminifera reappearing at the termination of the early  
496 Holocene (c. 9600 cal yr BP; Fig. 5). During this period, *N. pachyderma* (sin.) dominated, but  
497 certain peaks of *N. pachyderma* (dex.) and *T. quinqueloba* were noted. The two latter species  
498 are treated as subpolar species (Bé and Tolderlund, 1971), although *T. quinqueloba* also could  
499 be related to oceanic frontal conditions separating Atlantic and Arctic Water (Johannessen et  
500 al., 1994; Matthiessen et al., 2001). The peaks of *T. quinqueloba* near 9600 cal yr BP were

501 noted previously in the western Barents Sea margin (e.g., Hald et al., 2007; Risebrobakken et  
502 al., 2010).

503         Increasing foraminiferal biodiversity in Storfjordrenna (Fig. 5) as well as the  
504 occurrence of the thermophilous mollusc *Mytilus edulis* on the western Edgeøya (Salvigsen et  
505 al., 1992) suggest that the inflow of AW crossed Storfjordrenna and continued northward to  
506 the inner fjord by 9600 cal yr BP.

507

#### 508 **5.4 Glaciomarine unit II (mid-Holocene; 9200 cal yr BP to 3600 cal yr BP)**

509

510         The mid-Holocene was characterised by relatively stable environmental conditions,  
511 low sediment accumulation rates ( $0.002 \text{ g cm}^{-2}\text{yr}^{-1}$ ) and a slight delivery of IRD (Fig. 4),  
512 resulting from rather limited ice rafting and a reduced supply of fine-grained material to  
513 Storfjordrenna. Low sedimentation rates and the low Fe/Ca ratio reflect the reduced glacial  
514 conditions on Svalbard during the mid-Holocene (Elverhøi et al., 1995; Svendsen and  
515 Mangerud, 1997). In contrast, Hald et al. (2004) noted that in the record from Van  
516 Mijenfjorden, an enhanced tidewater glaciation occurred during this period; it was thus  
517 argued that IRD is a more reliable indicator of glaciation than sedimentation rates. However,  
518 ice rafting in Storfjordrenna was generally low.

519         Shifts between the dominant species *C. reniforme* and *E. excavatum* f. *clavata* (Fig. 5)  
520 reflect environmental/hydrological changes (Hald and Korsun, 1997). The decrease of *E.*  
521 *excavatum* f. *clavata* (percentage and flux), which prefers colder bottom waters (Sejrup et al.,  
522 2004; Saher et al., 2009) and the increase of *C. reniforme* point to the constant inflow of less  
523 modified AW and a reduction in sedimentation (e.g., Schröder-Adams et al., 1990; Bergsten,  
524 1994; Jennings and Helgadóttir, 1994; Hald and Steinsund, 1996; Hald and Korsun, 1997).  
525 Furthermore, the relative abundance of *M. barleeianum* (Fig. 5) indicates that environmental  
526 conditions in Storfjordrenna were similar to those of contemporary Norwegian fjords that are  
527 dominated by AW with a temperature of 6 - 8°C and salinities of 34 - 35 (Husum and Hald,  
528 2004). High total foraminiferal flux at the beginning of this period as well as high  
529 foraminiferal species richness and biodiversity clearly point to AW conditions at the bottom  
530 (Hald and Korsun, 1997; Majewski and Zajączkowski, 2007; Włodarska-Kowalczyk et al.,  
531 2013). These conclusions are also supported by the heavier  $\delta^{18}\text{O}$ , which demonstrates AW  
532 dominance and a significant reduction in the amount of freshwater and ArW in Storfjordrenna  
533 (Fig. 7). The reduced sea ice condition during the mid-Holocene was also observed on the  
534 northern Barents Sea continental margin seen as increase in paleoproductivity (Wollenburg et



535 al., 2004). The continuous presence of *Mytilus edulis* during the entire mid-Holocene points to  
536 the reduced inflow of the East Spitsbergen Current due to the AW inflow (Feyling-Hansen,  
537 1955; Forman, 1990; Salvigsen et al., 1992). The pathway and range of AW inflow to the  
538 western and northeastern Svalbard during mid-Holocene were well described by Ślubowska-  
539 Woldengen et al. (2008) and Groot et al. (2014). Taken together with our results, these  
540 observations suggest that one of the main pathways of AW inflow to the eastern Svalbard  
541 may have occurred through Storfjordrenna.

542 Although sediment accumulation rates were low and grain size and geochemical  
543 proxies remained relatively constant during the mid-Holocene, the foraminiferal flux  
544 (including planktonic foraminifera) increased in two periods of 9000 - 8000 cal yr BP and  
545 6000 - 5500 cal yr BP (Fig. 4 and 5, respectively). In both cases, the increase in IRD and *I.*  
546 *norcrossi* fluxes was followed by a slight depletion in  $\delta^{18}\text{O}$  and heavier  $\delta^{13}\text{C}$ , suggesting  
547 minor cooling and likely seasonal sea-ice formation leading to beach sediment transport by  
548 shore ice. Our observations support earlier studies of the overall mid-Holocene shifts towards  
549 a colder environment (Skirbekk et al., 2010; Rasmussen et al., 2012; Berben et al., 2014;  
550 Groot et al., 2014; Sternal et al., 2014) and fluctuations in the glacial activity in the Svalbard  
551 region (e.g., Forwick and Vorren, 2007, 2009; Beaten et al., 2010; Ojala et al., 2014). Our  
552 data show an increased supply of IRD fraction to the Storfjordrenna sediment followed by  
553 variation of  $\delta^{18}\text{O}$ ; however, the high flux of *M. barleeaanum* associated with Atlantic-derived  
554 waters (Steinsund, 1994; Jennings et al., 2004; Fig. 5) indicates an AW condition in southern  
555 Storfjorden throughout the entire mid-Holocene. A similar ameliorated condition with  
556 consistent AW inflow also prevailed over the mid-Holocene in the Kveithola Trough south of  
557 Storfjordrenna (Berben et al., 2014; Groot et al., 2014). To a lesser extent, these two signals  
558 (AW inflow and higher IRD flux) are not necessarily contradictory because snow  
559 accumulation on land and inconsiderable glacier advance depend on humid air transport from  
560 the ocean. Thus, slight changes in the atmospheric frontal zone over Svalbard could cause  
561 fluctuation of the glacier range.

562

### 563 **5.5 Glaciomarine unit III (late Holocene; 3600 cal yr BP to 1200 cal yr BP)**

564

565 The late Holocene is characterised by a gradual increase in sediment accumulation rates  
566 followed by numerous sharp peaks of sand content and minor peaks of IRD flux as well as an  
567 increased Fe/Ca ratio, thus indicating ice growth on land (compare with e.g., Svendsen and  
568 Mangerud, 1997; Hald et al., 2004; Forwick and Vorren, 2009; Kempf et al., 2013) and

569 slightly enhanced iceberg calving and/or ice rafting over the core site. The IRD record shows  
570 few irregular small peaks in the late Holocene (Fig. 6), which could be correlated with  
571 enhanced sea currents that increase the drift of the icebergs, according to Hass (2002).  
572 Forwick et al. (2010) suggested several glacier front fluctuations during the past two  
573 millennia in Sassenfjorden and Tempelfjorden (W Spitsbergen), and hence, we assume that  
574 increased iceberg calving occurred at Storfjordrenna during this time. However, increased  
575 IRD flux can also reflect deposition related to enhanced shore ice rafting. The latter  
576 explanation is in agreement with the heavier  $\delta^{18}\text{O}$  record (Fig. 5), indicating a minor cooling.

577 The mean grain size ( $<63\ \mu\text{m}$ ) increases in the late Holocene (Fig. 4) and may indicate  
578 stronger bottom current velocities and winnowing of fine-grained sediments. Andruleit et al.  
579 (1996) observed similar increased erosive activity of bottom currents during the late Holocene  
580 on the SW Svalbard shelf. This sudden increase in current velocities might be connected with  
581 (1) postglacial reorganisation of oceanographic conditions, (2) relative lowering of the sea  
582 level during the postglacial isostatic rebound and/or (3) more intensive sea-ice formation that  
583 enhanced the formation of BSW, thus forming a seasonal near-bottom dense water mass  
584 flowing over the coring site (Andruleit et al., 1996). Nevertheless, this process is still not fully  
585 understood.

586 The sharp increase in the foraminiferal flux (Fig. 4) pointing to the increased nutrient  
587 advection/upwelling and biological productivity at the coring site during the late Holocene  
588 was likely caused by variable hydrological conditions and most likely strong gradients leading  
589 to the formation of hydrological fronts. In contrast, Wollenburg et al. (2004) noted reduced  
590 paleoproductivity in the northern Barents Sea over the entire late Holocene, pointing to  
591 several events of heavy sea ice cover. Our data show increased fluxes of opportunistic species  
592 *E. excavatum* and *C. reniforme* as well as an abundance of *N. labradorica* and *Islandiella* spp.  
593 *N. labradorica* and *Islandiella* spp. in areas with a high biological productivity in the upper  
594 surface waters (e.g., Hald and Steinsund, 1996; Korsun and Hald, 2000; Knudsen et al.,  
595 2012). Abundant though variable *M. barleeianum* is documented in organic-rich mud within  
596 troughs of the Barents Sea (Hald and Steinsund, 1996) and in temperate fjords of Norway  
597 (Husum and Hald, 2004), which points to high productivity in the euphotic zone leading to  
598 enhanced export of organic material/nutrients to the sea floor. Our data also show high *N.*  
599 *pachyderma* flux throughout this unit, reflecting a significant increase of euphotic  
600 productivity at the coring site. However, a low percentage of dextral specimens and *T.*  
601 *quinqueloba* point to low sea-surface temperatures (Fig. 5). This observation is in agreement  
602 with Rasmussen et al. (2014), who noted that after c. 3700 cal yr BP, Atlantic Water was only

603 sporadically present at the surface. Cooling at the sea surface reflects the general trend in the  
604 Northern Hemisphere related to orbital forcing and reduction of summer insolation at high  
605 latitudes over the late Holocene (Wanner et al., 2008).

606 The last evidence of AW inflow to Edgøya area based on *M. edulis* is dated to 5000 cal yr  
607 BP (Hjort et al., 1995). After that time, *M. edulis* remained absent until the present time;  
608 however; its disappearance could be related to the freshening of Surface Water (Berge et al.,  
609 2006) and sea ice forcing as opposed to the extinction of AW in Storfjorden over the late  
610 Holocene (Rasmussen et al., 2007).

611

## 612 **6 Conclusions**

613

614 Multi-proxy analyses of one sediment core provide new information on the  
615 environmental development of the central portion of Storfjordrenna off the southern Svalbard  
616 since the late Bølling-Allerød. The main conclusions of our study are described as follows:

617 - Central Storfjordrenna was deglaciated prior to ~13,950 cal yr BP, and these new data may  
618 aid in refining future models of Svalbard-Barents Ice Sheet deglaciation.

619 - Between c. 13,450 to 11,500 cal yr BP, Storfjordrenna remained under the influence of  
620 Arctic Water masses with sea-ice cover episodically limiting the drift of icebergs.  
621 Nevertheless, at least three peaks in temperature that occurred during the Younger Dryas  
622 stadial (12,800-11,500 cal yr BP) presumably led to the seasonal disappearance of sea ice and  
623 significantly enhanced IRD flux, thus indicating more sub-polar conditions.

624 - Atlantic Water began to flow onto the shelves off Svalbard and into Storfjorden during the  
625 early Holocene, leading to progressive warming and significant glacial melting. From c. 9600  
626 cal yr BP, Atlantic Water dominated the water column in Storfjordrenna.

627 - The environmental conditions off eastern Svalbard remained relatively stable from 9200-  
628 3600 cal yr BP, with glaciers smaller than those of today. However, certain small-scale  
629 cooling events (9000 - 8000 cal yr BP and 6000 - 5500 cal yr BP) indicate minor fluctuations  
630 in the climate/oceanography of Storfjordrenna.

631 - A surface-water cooling and freshening occurred in Storfjordrenna during the late Holocene,  
632 synchronous with glacier growth and cooling on land and the presence of AW in the deeper

633 portion of Storfjordrenna. The late Holocene in Storfjordrenna experienced increased bottom  
634 current velocities; however, the driving mechanism is not fully understood.

635  
636 *Acknowledgements.* The study was supported by the Institute of Oceanology Polish Academy  
637 of Science and the Polish Ministry of Science and Higher Education with grant no. NN 306  
638 469938. The <sup>14</sup>C dating was funded by Polish Ministry of Science and Higher Education grant  
639 No. IP2010 040970. We thank the captain and crew of R/V Jan Mayen, as well as the cruise  
640 participants, in particular Steinar Iversen, for their help at sea. Trine Dahl and Ingvild Hald  
641 are acknowledged for the acquisition of X-radiographs. Tine Rasmussen (UiT) is gratefully  
642 acknowledged for sharing the data with us. Katarzyna Zamelczyk (UiT) and Maria  
643 Włodarska-Kowalczyk (IOPAS) are thanked for help in planktonic foraminifera (Katarzyna)  
644 and bivalves (Maria) determination. Patrycja Jernas (UiT) helped during subsampling of the  
645 cores. Master's students from the University of Gdansk Kamila Sobala and Anna Nowicka  
646 helped with the Mastersizer2000 analysis. We are highly grateful Renata Lucchi (Istituto  
647 Nazionale di Oceanografia e Geofisica Sperimentale, Italy), Reignheid Skogseth (University  
648 Centre in Svalbard) and Ilona Goszczko (IOPAS) for the comments on the early version of  
649 this manuscript. We are sincerely indebted to Amy Lusher (Galway-Mayo Institute of  
650 Technology), Sara Strey-Mellema (University of Illinois) and Christof Pearce (Stockholm  
651 University) for improving the English of this manuscript. The comments from two  
652 anonymous referees helped to improve the manuscript considerably.

## 653 **References**

- 654 Aagaard, K., Foldvik, A. and Hillman, S.: The West Spitsbergen Current: disposition and  
655 water mass transformation, *J. Geophys. Res.*, 92, 3778-3784, 1987.
- 656 Akimova, A., Schauer, U., Danilov, S. and Núñez-Riboni, I.: The role of the deep mixing in  
657 the Storfjorden shelf water plume, *Deep Sea Res. I*, 58, 403-414, 2011.
- 658 Alley, R.: The Younger Dryas cold interval as viewed from central Greenland, *Quat. Sci.*  
659 *Rev.*, 19 (1-5), 213-226, 2000.
- 660 Alley, R.B. and Augustdottir, A.M.: The 8 k event: cause and consequences of a major  
661 Holocene abrupt climate change, *Quat. Sci. Rev.*, 24, 1123-1149, 2005.
- 662 Alve, E. and Goldstein, S.T.: Dispersal, survival and delayed growth of benthic foraminiferal  
663 propagules, *J. Sea Res.*, 63(1), 36- 51, 2010.

664 Andreassen, K., Winsborrow, M., Bjarnadóttir, L.R. and Rüther, D.C.: Ice stream retreat  
665 dynamics inferred from an assemblage of landforms in the northern Barents Sea, *Quat. Sci.*  
666 *Rev.*, doi: 10.1016/j.quascirev.2013.09.015, 2014.

667 Andruleit, H., Freiwald, A. and Schäfer, P.: Bioclastic carbonate sediments on the  
668 southwestern Svalbard shelf, *Mar. Geol.*, 134, 163–182, 1996.

669 Baeten, N.J., Forwick, M., Vogt, C. and Vorren, T.O.: Late Weichselian and Holocene  
670 sedimentary environments and glacial activity in Billefjorden, Svalbard, In: Howe, J.A.,  
671 Austin, W.E.N, Forwick, M. and Paetzel, M. (Editors): *Fjord Systems and Archives*, *Geol.*  
672 *Soc. London Spec. Publ.*, 344, 207-223, 2010.

673 Bakke, J., Lie, Ø., Heegaard, E., Dokken, T., Haug, G.H., Birks, H.H., Dulski, P. and Nilsen,  
674 T.: Rapid oceanic and atmospheric changes during the Younger Dryas cold period, *Nat.*  
675 *Geosci.*, 2, 202-205, 2009.

676 Bauch, H.A., Erlenkeuser, H., Bauch, D., Mueller-Lupp, T. and Taldenkova, E.: Stable  
677 oxygen and carbon isotopes in modern benthic foraminifera from the Laptev Sea shelf:  
678 implications for reconstruction proglacial and profluvial environments in the Arctic, *Mar.*  
679 *Micropaleontol.*, 51, 285–300, 2004.

680 Bé, A.W.H. and D.S. Tolderlund: Distribution and ecology of living planktonic foraminifera  
681 in surface waters of the Atlantic and Indian oceans, in *The Micropaleontology of Oceans*,  
682 edited by B. M. Funnell and W. R. Riedel, pp. 105–149, Cambridge Univ. Press, Cambridge,  
683 U. K., 1971.

684 Berge, J., Johnsen, G., Nilsen, F., Gulliksen, B., Slagstad, D. and Pampanin, D.M.: The  
685 *Mytilus edulis* population in Svalbard: how and why, *Mar. Ecol. Prog. Ser.*, 309, 305-306,  
686 2006.

687 Bergsten, H.: Recent benthic foraminifera of a transect from the North Pole to the Yermak  
688 Plateau, eastern central Arctic Ocean, *Mar. Geol.*, 119 (3-4), 251-267, 1994.

689 Blott, S.J. and Pye, K.: GRADISTAT: a grain size distribution and statistics package for the  
690 analysis of unconsolidated sediments, *Earth Surf. Process. Landf.*, 26, 1237-1248, 2001.

691 Briner, J.P., Bini, A.C., and Anderson, R.S.: Rapid early Holocene retreat of a Laurentide  
692 outlet glacier through an Arctic fjord, *Nature Geosci.*, 2, 496-499, 2009.

693 Broecker, W.S.: Was the Younger Dryas triggered by a flood? *Science*, 312, 1146–1148, doi:  
694 10.1126/science.1123253, 2006.

695 Cronin, T.M., Rayburn, J.A., Guilbault, J.-P., Thunell, R. and Franzi, D.A.: Stable isotope  
696 evidence for glacial lake drainage through the St.Lawrence Estuary, eastern Canada, ~13.1-  
697 12.9 ka, *Quat. Sci. Rev.*, 260, 55-65, 2012.

698 Croudace, I. W., Rindby, A. and Rothwell, R. G.: ITRAX: description and evaluation of a  
699 new multi-function X-ray core scanner, *Geol. Soc. London, Spec. Publ.*, 267, 51–63, 2006.

700 Czernik, J. and Goslar, T.: Preparation of graphite targets in the Gliwice Radiocarbon  
701 Laboratory for AMS <sup>14</sup>C dating, *Radiocarbon*, 43, 283–291, 2001.

702 Dansgaard, W., Johnsen, S.J., Clausen, H.B., Dahl-Jensen, D., Gundestrup, N.S., Hammer, C.  
703 U.C., Hvidberg, S., Steffensen, J.P., Sveinbjörnsdóttir, A. E., Jouzel, J. and Bond G.:  
704 Evidence for general instability of past climate from a 250-kyr ice-core record, *Nature*, 364,  
705 218 – 220, doi:10.1038/364218a0, 1993.

706 Dowdeswell, J.A., Elverhøi, A. and Spielhagen, R.: Glacimarine sedimentary processes and  
707 facies on the polar north Atlantic margins, *Quat. Sci. Rev.*, 17, 243–272, 1998.

708 Duplessy, J.C., Cortijo, E., Ivanova, E., Khusid, T., Labeyrie, L., Levitan, M., Murdmaa, I.  
709 and Paterne, M.: Paleoceanography of the Barents Sea during the Holocene,  
710 *Paleoceanography*, 20(4), PA4004, doi: 10.1029/2004PA001116, 2005.

711 Dylmer, C.V., Giraudeau, J., Eynaud, F., Husum, K. and de Vernal, A.: Northward advection  
712 of Atlantic water in the eastern Nordic Seas over the last 3000 yr, *Clim. Past*, 9, 1505-1518,  
713 2013.

714 Eldevik, T., Risebrobakken, B., Bjune, A.E., Andersson, C., Birks, H.J.B., Dokken, T.M.,  
715 Drange, H., Glessmer, M.S., Li, C., Nilsen, J.E.Ø., Otterå, O.H., Richter, H. and Skagseth, Ø.:  
716 A brief history of climate e the northern seas from the Last Glacial Maximum to global  
717 warming, *Quat. Sci. Rev.*, 106, 225-246, 2014.

718 Elmore, A.C. and Wright, J.D: North Atlantic Deep Water and climate variability during the  
719 Younger Dryas cold period, *Geology*, 39:107, 2011.

720 Elverhøi, A., Svendsen, J.I., Solheim, A., Andersen, E.S., Milliman, J., Mangerud, J. and  
721 Hooke, R.L.: Late Quaternary Sediment Yield from the High Arctic Svalbard Area, *J. Geol.*,  
722 103, 1-17, 1995.

723 Fer, I., Skogseth, R., Haugan, P.M. and Jaccard, P.: Observations of the Storfjorden  
724 overflow, *Deep-Sea Res. I*, 50(10-11), 1283-1303, doi: 10.1016/S0967-0637(03)00124-9,  
725 2003.

726 Fer, I., Skogseth, R. and Haugan, P.M.: Mixing of the Storfjorden overflow (Svalbard  
727 Archipelago) inferred from density overturns, *J. Geophys. Res.*, 109,  
728 C01005, doi:10.1029/2003JC001968, 2004.

729 Feyling-Hanssen, R. and Jørstad, F.: Quaternary fossil from the Sassen-area in Isfjorden,  
730 west-Spitsbergen (the marine mollusk fauna), *Norsk Polarinstitutt Skrifter*, 94, 1-85, 1950.

731 Feyling-Hanssen, R.: Stratigraphy of the marine late-Pleistocene of Billefjorden,  
732 Vestspitsbergen, Norsk Polarinstittut Skrifter, 107, 1-186, 1955.

733 Forman, S.L.: Post-glacial relative sea level history of northwestern Spitsbergen, Svalbard, B.  
734 Geol. Soc. of America, 102, 1580–1590, 1990.

735 Forman, S.L., Lubinski, D.J., Ingólfsson, Ó., Zeeberg, J.J., Snyder, J.A., Siegert, M.J. and  
736 Matishov, G.G.: A review of postglacial emergence on Svalbard, Franz Josef Land and  
737 Novaya Zemlya, northern Eurasia, Quat. Sci. Rev., 23, 1391-1434, 2004.

738 Forwick, M. and Vorren, T.O.: Holocene mass-transport activity in and climate outer  
739 Isfjorden, Spitsbergen: marine and subsurface evidence, The Holocene, 17(6), 707-716, 2007.

740 Forwick, M. and Vorren, T.O.: Late Weichselian and Holocene sedimentary environments  
741 and ice rafting in Isfjorden, Spitsbergen, Palaeogeogr., Palaeoclim., Palaeoecol., 280, 258-  
742 274, 2009.

743 Forwick, M., Vorren, T.O., Hald, M., Korsun, S., Roh, Y., Vogt, C. and Yoo, K.-C.: Spatial  
744 and temporal influence of glaciers and rivers on the sedimentary environment in  
745 Sassenfjorden and Tempelfjorden, Spitsbergen. In: Howe, J.A., Austin, W.E.N, Forwick, M.  
746 and Paetzel, M. (Editors): Fjord Systems and Archives, Geol. Soc. London, Spec. Pub., 344,  
747 163-193, 2010.

748 Gammelsrod, T. and Rudels, B.: Hydrographic and current measurements in the Fram Strait,  
749 Pol. Res., 1, 115-126, 1983.

750 Geyer, F., Fer, I. and Smedsrud, L.: Structure and forcing of the overflow at the Storfjorden  
751 sill and its connection to the Arctic coastal polynya in Storfjorden, Ocean Sci. Disc., 7, 17-49,  
752 2010.

753 Gilbert, R.: Environmental assessment from the sedimentary record of highlatitude fiords,  
754 Geomorphology, 32, 295–314, 2000.

755 Gildor, H. and Tziperman, E.: A sea ice climate switch mechanism for the 100-kyr glacial  
756 cycles, J. Geophys. Res., 106, 9117-9133, 2001.

757 Goslar, T., Czernik, J. and Goslar, E.: Low-energy <sup>14</sup>C AMS in Poznań Radiocarbon  
758 Laboratory, Poland, Nucl. Instrum. Methods, B 223/224, 5–11, 2004.

759 Groot, D.E., Aagaard-Sørensen, S. and Husum, K.: Reconstruction of Atlantic water  
760 variability during the Holocene in the western Barents Sea, Clim. Past, 10, 51-62, 2014.

761 Grootes, P. M., Stuiver, M., White, J. W. C., Johnsen, S. J. and Jouzel, J.: Comparison of  
762 oxygen isotope records from the GISP2 and GRIP Greenland ice cores, Nature, London, 366,  
763 552-554, 1993.

764 Haarpaintner, J., Gascard, J. and Haugan, P.M.: Ice production and brine formation in  
765 Storfjorden, Svalbard, J. Geophys. Res., 106, doi: 10.1029/1999JC000133, 2001.

766 Hald, M., Ebbsen, H., Forwick, M., Godtliebsen, F., Khomenko, L., Korsun, S., Olsen, L.R.  
767 and Vorren, T.O.: Holocene paleoceanography and glacial history of the West Spitsbergen  
768 area, Euro-Arctic margin, Quat. Sci. Rev., 23, 2075-2088, 2004.

769 Hald, M. and Korsun, S.: Distribution of modern Arctic benthic foraminifera from fjords of  
770 Svalbard, J. Foramin. Res., 27, 101-122, 1997.

771 Hald, M. and Steinsund, P.I.: Benthic foraminifera and carbonate dissolution in surface  
772 sediments of the Barents-and Kara Seas, In: Stein, R., Ivanov, G.I., Levitan, M.A. and Fahl,  
773 K. (Editors), Surface-sediment composition and sedimentary processes in the central Arctic  
774 Ocean and along the Eurasian Continental Margin, Ber. Polarforsch., 212, 285-307, 1996.

775 Hald, M., Andersson, C., Ebbesen, H., Jansen, E., Klitgaard-Kristensen, D., Risebrobakken,  
776 B., Salomonsen, G.R., Sarnthein, M., Sejrup, H.P. and Telford, R.J.: Variations in  
777 temperature and extent of Atlantic Water in the Northern North Atlantic during the Holocene,  
778 Quat. Sci. Rev., 26, 3423–40, 2007.

779 Hald, M. and Korsun, S.: The 8200 cal. yr BP event reflected in the Arctic fjord, Van  
780 Mijenfjorden, Svalbard, The Holocene, 18, 981 – 990, doi: 10.1177/0959683608093536,  
781 2008.

782 Hansen, J., Hanken, N., Nielsen, J., Nielsen, J. and Thomsen, E.: Late Pleistocene and  
783 Holocene distribution of *Mytilus edulis* in the Barents Sea region and its paleoclimatic  
784 implications, J. Biogeogr., 38, 1197-1212, 2011.

785 Hass, H. C.: A method to reduce the influence of ice-rafted debris on a grain size record from  
786 northern Fram Strait, Polar Res., 21(2), 299-306, 2002.

787 Hjort, C., Adrielsson, L., Bondevik, S., Landvik, J., Mangerud, J. and Salvigsen, O.: *Mytilus*  
788 *edulis* on eastern Svalbard- dating the Holocene Atlantic Water influx maximum, Lundqua  
789 Rep., 35, 171-175, 1992.

790 Hjort, C., Mangerud, J., Adrielsson, L., Bondevik, S., Landvik, J. Y. and Salvigsen, O.:  
791 Radiocarbon dated common mussels *Mytilus edulis* from eastern Svalbard and the Holocene  
792 marine climatic optimum, Polar Res., 14(2), 239–243, 1995.

793 Hormes, A., Gjermundsen, E.F. and Rasmussen, T.L.: From mountain top to the deep sea -  
794 deglaciation in 4D of the northwestern Barents Sea, Quat. Sci. Rev., 75, 78-99, 2013.

795 Husum, K. and Hald, M.: A continuous marine record 8000-1600 cal. yr BP from the  
796 Malangenfjord, north Norway: foraminiferal and isotopic evidence, The Holocene, 14, 877 –  
797 887, 2004.



798 Jennings, A.E., Knudsen, K.L., Hald, M., Hansen, C.V. and Andrews, J.T.: A mid-Holocene  
799 shift in Arctic sea-ice variability on the East Greenland Shelf, *The Holocene*, 12 (1), 49-58,  
800 2002.

801 Jennings, A.E. and Helgadottir, G.: Foraminiferal assemblages from the fjords and shelf of  
802 Eastern Greenland, *J. Foramin. Res.*, 24, 123–44, 1994.

803 Jennings, A.E., Hald, M., Smith, M., and Andrews, J.T.: Freshwater forcing from the  
804 Greenland Ice Sheet during the Younger Dryas: evidence from southeastern Greenland shelf  
805 cores, *Quat. Sci. Rev.*, 25, 282-298, 2004.

806 Jennings, A.E., Hald, M., Smith, M., and Andrews, J.T.: Freshwater forcing from the  
807 Greenland Ice Sheet during the Younger Dryas: evidence from southeastern Greenland shelf  
808 cores, *Quat. Sci. Rev.*, 25, 282-298, 2006.

809 Jessen, S.P., Rasmussen, T.L., Nielsen, T. and Solheim, A.: A New Late Weichselian And  
810 Holocene Marine Chronology For The Western Svalbard Slope 30,000 - 0 Cal Years BP,  
811 *Quat. Sci. Rev.*, 29 (9-10), 1301 – 1312, doi: 10.1016/j.quascirev.2010.02.020, 2010.

812 Johannessen, T., Jansen, E., Flatøy, A. and Ravelo, A.C.: The relationship between surface  
813 water masses, oceanographic fronts and paleoclimatic proxies in surface sediments of the  
814 Greenland, Iceland, Norwegian Seas, In Zahn, R., Kominski, M. and Labyrie, L., editors,  
815 *Carbon cycling in glacial ocean: constraints on the ocean's role in global change*. Springer-  
816 Verlag, 61–85, 1994.

817 Kaufman, D. S., Ager, T. A., Anderson, N. J., Anderson, P. M., Andrews, J. T., Bartlein, P. J.,  
818 Brubaker, L. B., Coats, L. L., Cwynar, L. C., Duvall, M. L., Dyke, A. S., Edwards, M. E.,  
819 Eisner, W. R., Gajewski, K., Geirsdóttir, A., Hu, F. S., Jennings, A. E., Kaplan, M. R.,  
820 Kerwin, M. W., Lozhkin, A. V., MacDonald, G. M., Miller, G. H., Mock, C. J., Oswald, W.  
821 W., Otto-Bliesner, B. L., Porinchu, D. F., Rühland, K., Smol, J. P., Steig, E. J. and Wolfe, B.  
822 B.: Holocene thermal maximum in the western Arctic (0-180°W), *Quat. Sci. Rev.*, 23 (5-6),  
823 529 – 560, 2004.

824 Kempf, P., Forwick, M., Laberg, J.S. and Vorren, T.O.: Late Weichselian – Holocene  
825 sedimentary palaeoenvironment and glacial activity in the high-Arctic van Keulenfjorden,  
826 Spitsbergen, *The Holocene*, 23, 1605-1616, 2013.

827 Klitgaard Kristensen, D., Rasmussen T.L. and Koç, N.: Palaeoceanographic changes in the  
828 northern Barents Sea during the last 16 000 years- new constraints on the last deglaciation of  
829 the Svalbard-Barents Sea Ice Sheet, *Boreas*, 42, 798-813, 2013.

830 Knudsen, K. L., Eiríksson, J. and Bartels-Jónsdóttir, H. B.: Oceanographic changes through  
831 the last millennium off North Iceland: Temperature and salinity reconstructions based on  
832 foraminifera and stable isotopes, *Mar. Micropaleontol.*, 54–73, 2012.

833 Korsun, S. and Hald, M.: Modern benthic foraminifera off tide water glaciers, Novaja Semlja,  
834 Russian Arctic, *Arctic Alpine Res.*, 30 (1), 61-77, 1998.

835 Korsun, S. and Hald, M.: Seasonal dynamics of benthic foraminifera in a glacially fed fjord of  
836 Svalbard, European Arctic, *J. Foramin. Res.*, 30(4), 251-271, 2000.

837 Kubischta, F., Knudsen, K. L., Kaakinen, A. and Salonen, V.-P.: Late Quaternary  
838 foraminiferal record in Murchisonfjorden, Nordaustlandet, Svalbard, *Polar Res.*, 29, 283–297,  
839 2010.

840 Landvik, J.Y., Hjort, C., Mangerud, J., Möller, P. and Salvigsen, O.: The Quaternary record of  
841 eastern Svalbard: an overview, *Polar Res.*, 14, 95-103, 1995.

842 Lloyd, J.M., Park, L.A., Kuijpers, A. and Moros, M.: Early Holocene palaeoceanography and  
843 deglacial chronology of Disko Bugt, West Greenland, *Quat. Sci. Rev.*, 24, 1741-1755, 2005.

844 Loeblich, A.R. and Tappan, H.: *Foraminiferal Genera and Their Classification*, Van Nostrand  
845 Reinhold, New York, 970, 1987.

846 Loeng, H.: Features of the physical oceanographic conditions of the Barents Sea, *Polar Res.*,  
847 10, 5–18, 1991.

848 Lubinski, D. J., Forman, S. L. and Miller, G. H.: Holocene glacier and climate fluctuations on  
849 Franz Josef Land, Arctic Russia, 80°N, *Quat. Sci. Rev.*, 18, 85-108, 1999.

850 Lucchi, R.G., Camerlenghi, A., Rebesco, M., Colmenero-Hidalgo, E., Sierro, F.J., Sagnotti,  
851 L., Urgeles, R., Melis, R., Morigi, C., Bárcena, M.-A., Giorgetti, G., Villa, G., Persico, D.,  
852 Flores, J.-A., Rigual-Hernández, A.S., Pedrosa, M.T., Macri, P. and Caburlotto, A.:  
853 Postglacial sedimentary processes on the Storfjorden and Kveithola trough mouth fans:  
854 Significance of extreme glacial sedimentation, *Global Planet. Change*, 111, 309-326, 2013.

855 Lydersen, C., Nøst, O., Lovell, P., McConell, B., Gammelsrød, T., Hunter, C., Fedak, M. and  
856 Kovacs, K.: Salinity and temperature structure of a freezing Arctic fjord- monitored by white  
857 whales (*Delphinapterus leucas*), *Geophys. Res. Lett.*, 29, doi: 10.1029/2002GL015462, 2002.

858 Majewski, W. and Zajączkowski, M.: Benthic foraminifera in Adventfjorden, Svalbard: Last  
859 50 years of local hydrographic changes, *J. Foramin. Res.*, 37, 107-124, 2007.

860 Mangerud, J., Bondevik, S., Gulliksen, S., Hufthammer, A.K. and Høisæter, T.: Marine <sup>14</sup>C  
861 reservoir ages for 19<sup>th</sup> century whales and molluscs from the North Atlantic, *Quat. Sci. Rev.*,  
862 25, 3228-3245, 2006.

863 Matthiessen, J., Baumann, K.H., Schröder-Ritzrau, A., Hass, C., Andrulleit, H., Baumann, A.,  
864 Jensen, S., Kohly, A., Pflaumann, U., Samtleben, C., Schäfer, P. and Thiede, J.: Distribution  
865 of calcareous, siliceous and organic-walled planktic microfossils in surface sediments of the  
866 Nordic seas and their relation to surface-water masses, In Schäfer, P., Ritzrau, W., Schlüter,  
867 M. and Thiede, J., editors, *The northern North Atlantic: a changing environment*. Springer,  
868 105–27, 2001.

869 Mayewski, P.A., Meeker, L.D., Morrison, M.C., Twickler, M.S., Whitlow, S.I., Ferland,  
870 K.K., Meese, D.A., Legrand, M.R. and Steffensen, J.P.: Greenland ice core “signal”  
871 characteristics: An expanded view of climate change, *J. Geophys. Res.*, 98, doi:  
872 10.1029/93JD01085, 1993.

873 McCarthy, D.J.: *Late Quaternary Ice-ocean Interactions in Central West Greenland*,  
874 Department of Geography, Durham University, Durham, UK, 2011.

875 Munsell® Color Geological Rock-Color Chart Revised Washable Edition, 2009.

876 Murton, J.B., Bateman, M.D., Dallimore, S.R., Teller, J.T. and Yang, Z.: Identification of  
877 Younger Dryas outburst flood path from Lake Agassiz to the Arctic Ocean, *Nature*, 464, 740-  
878 743, 2010.

879 Norges Sjøkartverk: *Den norske los- Arctic pilot, Farvannbeskrivelse, sailing directions*,  
880 Svalbard-Jan Mayen, Seventh edition, Stavanger, Norwegian Hydrographic Service,  
881 Norwegian Polar Institute, 1988.

882 O'Dwyer, J., Kasajima, Y., and Nøst, O.: North Atlantic water in the Barents Sea opening,  
883 1997 to 1999, *Polar Res.*, 2, 209–216, 2001.

884 Ojala, A.E. K., Salonen, V.-P., Moskalik, M., Kubischta, F. and Oinonen, M.: Holocene  
885 sedimentary environment of a High-Arctic fjord in Nordaustlandet, Svalbard, *Pol. Polar Res.*,  
886 03, 35(1), 73-98, 2014.

887 Østby, K. L. and Nagy, J.: Foraminiferal Distribution in the Western Barents Sea, Recent and  
888 Quaternary, *Polar Res.*, 1, 55–95, 1982.

889 Osterman, L.E. and Nelson, A.R.: Latest Quaternary and Holocene paleoceanography of the  
890 eastern Baffin Island continental shelf, Canada: benthic foraminiferal evidence, *Can. J. Earth*  
891 *Sci.*, 26(11), 2236-2248, 1989.

892 Ottesen, D., Dowdeswell, J.A. and Rise, L.: Submarine landforms and the reconstruction of  
893 fast-flowing ice streams within a large Quaternary ice sheet: the 2500-km-long Norwegian–  
894 Svalbard margin (57°–80°N), *Geol. Soc. Am. Bull.*, 117, 1033–1050, 2005.

895 Pearce, C., Seidenkrantz, M.-S., Kuijpers, A., Massé, G., Reynisson, N.F. and Kristiansen,  
896 S.M.: Ocean lead at the termination of the Younger Dryas cold spell, *Nature Comm.*, 4, 1664,  
897 2013.

898 Pedrosa, M. T., Camerlenghi, A., de Mol, B., Urgeles, R., Rebesco, M., Lucchi, R. G.,  
899 Amblas, D., Calafat, A., Canals, M., Casamor, J. L., Costa, S., Frigola, J., Iglesias, O.,  
900 Lafuerza, S., Lastras, G., Lavoie, C., Liqueste, C., Hidalgo, E. C., Flores, J. A., Sierro, F. J.,  
901 Carburlotto, A., Grossi, M., Winsborrow, M., Zgur, F., Deponte, D., De Vittor, C., Facchin,  
902 L., Tomini, I., De Vittor, R., Pelos, C., Persissinotto, G., Ferrante, N. and Di Curzio, E.:  
903 Seabed morphology and shallow sedimentary structure of the Storfjorden and Kveithola  
904 trough-mouth fans northwest Barents Sea, *Mar. Geol.*, 286, 1-4, 2011.

905 Piechura, J.: Dense bottom waters in Storfjord and Storfjordrenna, *Oceanologia*, 38, 285-292,  
906 1996.

907 Polyak, L. and Mikhailov, V.: Post-glacial environments of the southeastern Barents Sea:  
908 Foraminiferal evidence, *Geol. Soc. London, Spec. Publ.*, 111, 323-337, 1996.

909 Polyak, L. and Solheim, A.: Late- and post-glacial environments in the northern Barents Sea  
910 west of Franz Josef Land, *Polar Res.*, 13, 97-207, 1994.

911 Quadfasel, D., Rudels, B., and Kurz, K.: Outflow of dense water from a Svalbard fjord into  
912 the Fram Strait, *Deep-Sea Res.*, 35, 1143-1150, 1988.

913 Quadfasel, D. A., Sy, A., Wells, D. and Tunik, A.: Warming in the Arctic, *Nature*, 350, 385,  
914 1991.

915 Rasmussen, T., L., Thomsen, E., Slubowska-Woldengen, M., Jessen, S., Solheim, A. and  
916 Koc, N.: Paleoceanographic evolution of the SW Svalbard margin (76°N) since 20,000 <sup>14</sup>C yr  
917 BP, *Quat. Res.*, 67, 100-114, doi: 10.1016/j.yqres.2006.07.002, 2007.

918 Rasmussen, T.L. and Thomsen, E.: Stable isotope signals from brines in the Barents Sea:  
919 Implications for brine formation during the last glaciation, *Geology*, 37 (10), 903 – 906, doi:  
920 10.1130/G25543A.1, 2009.

921 Rasmussen, T.L., Forwick, M. and Mackensen, A.: Reconstruction of inflow of Atlantic  
922 Water to Isfjorden, Svalbard during the Holocene: Correlation to climate and seasonality,  
923 *Mar. Micropaleontol.*, 94-95, 80 – 90, doi: 10.1016/j.marmicro.2012.06.008, 2012.

924 Rasmussen, T.L., Thomsen, E., Skirbekk, K., Ślubowska-Woldengen, M., Klitgaard  
925 Kristensen, D. and Koç, N.: Spatial and temporal distribution of Holocene temperature  
926 maxima in the northern Nordic seas: interplay of Atlantic-, Arctic- and polar water masses,  
927 *Quat. Sci. Rev.*, 92, 280-291, <http://dx.doi.org/10.1016/j.quascirev.2013.10.034>, 2014.

928 Rasmussen, T.L. and Thomsen, E.: Brine formation in relation to climate changes and ice  
929 retreat during the last 15,000 years in Storfjorden, Svalbard, 76–78°N, *Paleoceanography*, doi:  
930 10.1002/2014PA002643, 2014.

931 Rasmussen, T.L. and Thomsen, E.: Palaeoceanographic development in Storfjorden,  
932 Svalbard, during the deglaciation and Holocene: evidence from benthic foraminiferal records,  
933 *Boreas*, doi: 10.1111/bor.12098, 2014.

934 Reimer, P.J., Bard, E., Bayliss, A., Beck, J.W., Blackwell, P.G., Bronk Ramsey, C., Buck,  
935 C.E., Cheng, H., Edwards, R.L., Friedrich, M., Grootes, P.M., Guilderson, T.P., Haflidason,  
936 H., Hajdas, I., HattĀš, C., Heaton, T.J., Hogg, A.G., Hughen, K.A., Kaiser, K.F., Kromer, B.,  
937 Manning, S.W., Niu, M., Reimer, R.W., Richards, D.A., Scott, E.M., Southon, J.R., Turney,  
938 C.S.M. and van der Plicht, J.: IntCal13 and MARINE13 radiocarbon age calibration curves 0-  
939 50000 years cal BP, *Radiocarbon* 55(4), 2013, doi: 10.2458/azu\_js\_rc.55.16947

940 Risebrobakken, B., Moros, M., Ivanova, E. V., Chistyakova, N., and Rosenberg, R.: Climate  
941 and oceanographic variability in the SW Barents Sea during the Holocene, *The Holocene*, 20,  
942 609–621, doi:10.1177/0959683609356586, 2010.

943 Risebrobakken, B., Dokken, T., Smedsrud, L., Andersson, C., Jansen, E., Moros, M., and  
944 Ivanova, E.: Early Holocene temperature variability in the Nordic Seas: The role of oceanic  
945 heat advection versus changes in orbital forcing, *Paleoceanography*, 26, PA4206,  
946 doi:10.1029/2011PA002117, 2011.

947 R  ther, D., Bjarnad  ttir, L.,R., Junttila, J., Husum, K., Rasmussen, T.L., Lucchi, R., G. and  
948 Andreassen, K.: Pattern and timing of the northwestern Barents Sea Ice Sheet deglaciation  
949 and indications of episodic Holocene deposition, *Boreas*, 41(3), 494-512, doi:10.1111/j.1502-  
950 3885.2011.00244.x, 2012.

951 Saher, M.H., Klitgaard Kristensen, D., Hald, M., Korsun, S. and J  rgensen, L.L.: Benthic  
952 foraminifera assemblages in the Central Barents Sea: an evaluation of the effect of combining  
953 live and total fauna studies in tracking environmental change, *Norw. J. Geol.*, 89, 149-161,  
954 2009.

955 Salvigsen, O., Forman S. and Miller, G.: Thermophilous mollusks on Svalbard during the  
956 Holocene and their paleoclimatic implications, *Polar Res.*, 11, 1-10, 1992.

957 Sarnthein, M., van Kreveld, S., Erlenkeuser, H., Grootes, P.M., Kucera, M., Pflaumann, U.  
958 and Sculz, M.: Centennial-to-millennial-scale periodicities of Holocene climate and sediment  
959 injections off the western Barents shelf, 75°N, *Boreas*, 32, 447-461, 2003.

960 Schauer, U.: The release of brine-enriched shelf water from Storfjord into the Norwegian Sea,  
961 *J. Geophys. Res.-Oceans*, 100, 60515-16028, 1995.

962 Schauer, U. and Fahrbach, E.: A dense bottom water plume in the western Barents Sea:  
963 Downstream modification and interannual variability, *Deep-Sea Res. I*, 46, 2095-2108, 1999.

964 Schauer, U., Fahrbach, E., Østerhus, S. and Rohardt, G.: Arctic Warming through the Fram  
965 Strait: Oceanic heat transport from 3 years of measurements, *J. Geophys. Res.*, 109, C06026,  
966 2004.

967 Schröder-Adams, C.J., Cole, F.E., Medioli, F.S., Mudie, P.J., Scott, D.B., and Dobbin, L.:  
968 Recent Arctic shelf foraminifera: Seasonally ice covered areas vs. perennially ice covered  
969 areas, *J. Foramin. Res.*, 20(1), 8 – 36, 1990.

970 Sejrup, H.P., Birks, H.J.B., Kristensen, D.K. and Madsen, H.: Benthonic foraminiferal  
971 distributions and quantitative transfer functions for the northwest European continental  
972 margin. *Mar. Micropaleontolog.*, 53 (1-2), 197 – 226, 10.1016/j.marmicro.2004.05.009, 2004.

973 Serreze, M. C., Maslanik, J. A., Scambos, T. A., Fetterer, F., Stroeve, J., Knowles, K.,  
974 Fowler, C., Drobot, S., Barry R. G. and Haran., T. M.: A new record minimum Arctic sea ice  
975 and extent in 2002, *Geophys. Res. Lett.*, 30, 1110, doi:10.1029/2002GL016406, 2003.

976 Siegert, M.J. and Dowdeswell, J.A.: Late Weichselian iceberg, surface-melt and sediment  
977 production from the Eurasian Ice Sheet: results from numerical ice sheet modeling, *Mar.*  
978 *Geol.*, 188, 109-127, 2002.

979 Skirbekk, K., Klitgaard Kristensen, D., Rasmussen, T., Koç, N. and Forwick, M.: Holocene  
980 climate variations at the entrance to a warm Arctic fjord: evidence from Kongsfjorden  
981 Trough, Svalbard, In: Howe, J.A., Austin, W.E.N, Forwick, M. and Paetzel, M.  
982 (Editors): *Fjord Systems and Archives*, *Geol. Soc. London, Spec. Publ.*, 344, 289-304, 2010.

983 Skogseth, R., Haugan, P. M. and Haarpaintner, J.: Ice and brine production in Storfjorden  
984 from four winters of satellite and in situ observations and modeling, *J. Geophys. Res.*, 109  
985 (C10), doi: 10.1029/2004JC002384, 2004.

986 Skogseth, R., Haugan, P. M. and Jakobsson, M.: Watermass transformations in Storfjorden,  
987 *Cont. Shelf Res.*, 25, 667–695, 2005.

988 Ślubowska, M.A., Koç, N., Rasmussen, T.L. and Klitgaard-Kristensen, D.: Changes in the  
989 flow of Atlantic water into the Arctic Ocean since the last deglaciation: Evidence from the  
990 northern Svalbard continental margin, 80°N, *Paleoceanography*, 20, 1-16, doi:  
991 10.1029/2005PA001141, 2005.

992 Ślubowska-Woldengen, M., Rasmussen, T.L., Koç, N., Klitgaard-Kristensen, D., Nilsen, F.  
993 and Solheim, A.: Advection of Atlantic Water to the western and northern Svalbard shelf  
994 since 17,500 cal yr BP, *Quat. Sci. Rev.*, 26, 463-478, doi: 10.1016/j.quascirev.2006.09.009,  
995 2007.

996 Ślubowska-Woldengen, M., Koç, N., Rasmussen, T.L., Klitgaard-Kristensen, D., Hald, M.  
997 and Jennings, A.E.: Time-slice reconstructions of ocean circulation changes on the continental  
998 shelf in the Nordic and Barents Seas during the last 16,000 cal yr B.P., *Quat. Sci. Rev.*, 27,  
999 1476 – 1492, doi: 10.1016/j.quascirev.2008.04.015, 2008.

1000 Smedsrud, L. H., Esau, I., Ingvaldsen, R. B., Eldevik, T., Haugan, P. M. and co-authors: The  
1001 role of the Barents Sea in the Arctic climate system, *Rev. Geophys*, 51, 415-449, 2013.

1002 Spielhagen, R.F., Werner, K., Sørensen, S.A., Zamelczyk, K., Kandiano, E., Budéus, G.,  
1003 Husum, K., Marchitto, T.M. and Hald, M.: Enhanced Modern Heat Transfer to the Arctic by  
1004 Warm Atlantic Water, *Science*, 331 (6016), 450 – 453, doi: 10.1126/science.1197397, 2011.

1005 Steinsund, P.I.: Benthic foraminifera in surface sediments of the Barents and Kara seas:  
1006 modern and late Quaternary applications, PhD thesis, University of Tromsø, 1994.

1007 Sternal, B., Szczuciński, W., Forwick, M., Zajączkowski, M., Lorenc, S. and Przytarska, J.:  
1008 Postglacial variability in near-bottom current speed on the Continental shelf off south-west  
1009 Spitsbergen, *J. Quat. Sci.*, 29(8), 767-777.

1010 Stuiver, M., Grootes, P.M. and Braziunas, T.F.: The GISP2 <sup>18</sup>O climate record of the past  
1011 16,500 years and the role of the sun, ocean and volcanoes, *Quat. Res.*, 44, 341-354, 1995.

1012 Stuiver, M. and Reimer, P. J.: Extended <sup>14</sup>C database and revised CALIB radiocarbon  
1013 calibration program, *Radiocarbon*, 35, 215–230, 1993.

1014 Stuiver, M., Reimer, P. J., and Reimer, R. W.: CALIB 5.0. [WWW program and  
1015 documentation], 2005.

1016 Svendsen, J. I., Elverhøi, A. and Mangerud, J.: The retreat of the Barents Sea Ice Sheet on the  
1017 western Svalbard margin, *Boreas*, 25, 244-256, 1996.

1018 Svendsen, J. I. and Mangerud, J.: Holocene glacial and climatic variations on Spitsbergen,  
1019 Svalbard, *The Holocene*, 7, 45-57, 1997.

1020 Svendsen, H., Beszczynska-Møller, A., Hagen, J.O., Lefauconnier, B., Tverberg, V., Gerland,  
1021 S., Ørebæk J.B., Bischof, K., Papucci, C., Zajączkowski, M., Azzolini, R., Bruland, O.,  
1022 Wiemcke, C., Winther, J.-G. and Dallmann, W.: The physical environment of Kongsfjorden-  
1023 Krossfjorden, an Arctic fjord system in Svalbard, *Polar Res.*, 21, 1, 133-166, 2002.

1024 Szczuciński, W., Zajączkowski, M. and Scholten, J.: Sediment accumulation rates in subpolar  
1025 fjords - impact of post-Little Ice Age glaciers retreat, Billefjorden, Svalbard, *Estuarine Coast.  
1026 Shelf Sci.*, 85, 345-356, 2009.

1027 Thorarinsdóttir, G. and Gunnarson, K.: Reproductive cycles of *Mytilus edulis* L. on the west  
1028 and east coast of Iceland, *Polar Res.*, 22, 217-223, 2003.

1029 Vilks, G.: Late glacial-postglacial foraminiferal boundary in sediments of eastern Canada,  
1030 Denmark and Norway, *Geosci. Canada*, 8, 48-55, 1981.

1031 Walczowski, W. and Piechura, J.: New evidence of warming propagating toward the Arctic  
1032 Ocean, *Geophys. Res. Lett.*, 33, L12601, doi:10.1029/2006GL025872, 2006.

1033 Walczowski, W. and Piechura, J.: Pathways of the Greenland Sea warming, *Geophys. Res.*  
1034 *Lett.*, 34, L10608, doi:10.1029/2007GL029974, 2007.

1035 Walczowski, W., Piechura, J., Goszczko, I. and Wieczorek, P.: Changes in Atlantic water  
1036 properties: an important factor in the European Arctic marine climate, *ICES J. Mar. Sci.*,  
1037 69(5), 864–869, doi:10.1093/icesjms/fss068, 2012.

1038 Wanner, H., Beer, J., Bütikofer, J., Crowley, T.J., Cubasch, U., Flückiger, J., Goosse, H.,  
1039 Grosjean, M., Joos, F., Kaplan, J.O., Küttel, M., Müller, S., Prentice, I.C., Solomina, O.,  
1040 Stocker, T.F., Tarasov, P., Wagner, M. and Widmann, M.: Mid- to late Holocene climate  
1041 change: an overview, *Quat. Sci. Rev.*, 27, 1791-1828, 2008.

1042 Weber, M.E., Niessen, F., Kuhn, G. and Wiedicke-Hombach, M.: Calibration and application  
1043 of marine sedimentary physical properties using a multi-sensor core logger, *Mar. Geol.*,  
1044 136(3-4), 151-172, doi:10.1016/S0025-3227(96)00071-0, 1997.

1045 Werner, K., Spielhagen, R. F., Bauch, D., Hass, H. C., Kandiano, E. S. and Zamelczyk, K.:  
1046 Atlantic Water advection to the eastern Fram Strait - multiproxy evidence for late Holocene  
1047 variability, *Palaeogeogr., Palaeoclim., Palaeoecol.*, 308(3-4), 264-276, 2011.

1048 Winkelmann, D. and Knies, J.: Recent distribution and accumulation of organic carbon on the  
1049 continental margin west off Spitsbergen, *Geochem., Geophys., Geosyst.*, 6(9), Q09012,  
1050 doi:10.1029/2005GC000916, 2005.

1051 Winsborrow, M.C.M., Andreassen, K., Corner, G.D. and Laberg, J.S.: Deglaciation of a  
1052 marine-based ice sheet: Late Weichselian Palaeo-ice dynamics and retreat in the southern  
1053 Barents Sea reconstructed from onshore and offshore glacial geomorphology, *Quat. Sci. Rev.*  
1054 29 (3-4), 424-442, 2010.

1055 Witus, A.E., Branecky, C.M., Anderson, J.B., Szczuciński, W., Schroeder, D.D. and  
1056 Jakobsson, M.: Meltwater intensive glacial retreat in polar environments and investigation of  
1057 associated sediments: example from Pine Island Bay, West Antarctica, *Quat. Sci. Rev.*, 85,  
1058 99-118, 2014.

1059 Włodarska-Kowalczyk, M., Pawłowska, J. and Zajączkowski, M.: Do foraminifera mirror  
1060 diversity and distribution patterns of macrobenthic fauna in an Arctic glacial fjord? *Mar.*  
1061 *Micropaleontol.*, 103, 30-39, 2013.



1062 Wollenburg, J.E., Knies, J. and Mackensen, A.: High-resolution paleoproductivity  
1063 fluctuations during the past 24 kyr as indicated by benthic foraminifera in the marginal Arctic  
1064 Ocean, *Palaeogeogr., Palaeoclim., Palaeoecol.*, 204, 209-238, 2004.

1065 Zajączkowski, M., Szczuciński, W. and Bojanowski, R.: Recent sediment accumulation rates  
1066 in Adventfjorden, Svalbard, *Oceanologia*, 46, 217-231, 2004.

1067 Zajączkowski, M., Nygård, H., Hegseth, E.N. and Berge, J.: Vertical flux of particulate matter  
1068 in an Arctic fjord: the case of lack of the sea-ice cover in Adventfjorden 2006 – 2007, *Polar*  
1069 *Biology*, 33, 223-239, 2010.

1070 Zamelczyk, K., Rasmussen, T.L., Husum, K., Haflidason, H., de Vernal, A., Ravna, E.K.,  
1071 Hald, M. and Hillaire-Marcel, C.: Paleoceanographic changes and calcium carbonate  
1072 dissolution in the central Fram Strait during the last 20 ka, *Quat. Res.*, 78, 405-416, 2012.

1073  
1074  
1075  
1076  
1077  
1078  
1079  
1080  
1081  
1082  
1083  
1084  
1085  
1086  
1087  
1088  
1089  
1090  
1091  
1092  
1093  
1094  
1095

1096 **Table 1**

1097 Water mass characteristics in Storfjorden and Storfjordrenna (Skogseth et al., 2005,  
 1098 modified). The two main water masses are in bold.

Watermass names	Watermass characteristics	
	Temperature (°C)	Salinity
<b>Atlantic Water (AW)</b>	<b>&gt;3.0</b>	<b>&gt;34.95</b>
<b>Arctic Water (ArW)</b>	<b>&lt;0.0</b>	<b>34.3-34.8</b>
Brine-enriched Shelf Water (BSW)	<-1.5	>34.8
Surface Water (SW)	>0.0	<34.4
Transformed Atlantic Water (TAW)	>0.0	>34.8

1099

1100

1101

1102

1103

1104

1105

1106

1107

1108

1109

1110

1111

1112 **Table 2**

1113 AMS <sup>14</sup>C dates and calibrated ages.

<i>Sample No</i>	<i>Depth [cm]</i>	<i>Lab No.</i>	<i>Raw AMS <sup>14</sup>C BP</i>	<i>Calibrated years BP ± 2σ</i>	<i>Cal yr BP used in age model</i>	<i>Dated material</i>
St 20A 5/6	5	Poz-46955	1835 ± 30 BP	1200 – 1365	1285	<i>Cilliatocardium cilliatum</i>
St 20A 39	38.5	Poz-46957	2755 ± 30 BP	2245 – 2470	Not used	<i>Astarte crenata</i>
St 20 78/79	78	Poz-46958	2735 ± 30 BP	2177 – 2429	2320	<i>Astarte crenata</i>
St 20 110	109.5	Poz-46959	3450 ± 30 BP	3079 – 3323	3220	<i>Astarte crenata</i>
St 20 142	141.5	Poz-46961	6580 ± 40 BP	6850 – 7133	6970	<i>Astarte crenata</i>
St 20A 152	151.5	Poz-46962	7790 ± 40 BP	8018 – 8277	8160	<i>Astarte crenata</i>
St 20 157	156.5	Poz-46963	8610 ± 50 BP	8989 – 9288	9120	<i>Batharca glacialis</i>
St 20 251/252/253	252	Poz-46964	10,200 ± 60 BP	10,895 – 11,223	11,230	<i>Thracia sp</i>
St 20 396	395.5	Poz-46965	12,570 ± 60 BP	13,780 – 14,114	13,950	Bivalvia shell

1114

1115

1116

1117

1118

1119

1120

1121

1122

1123

1124

1125

1126

1127

1128

1129

1130

1131

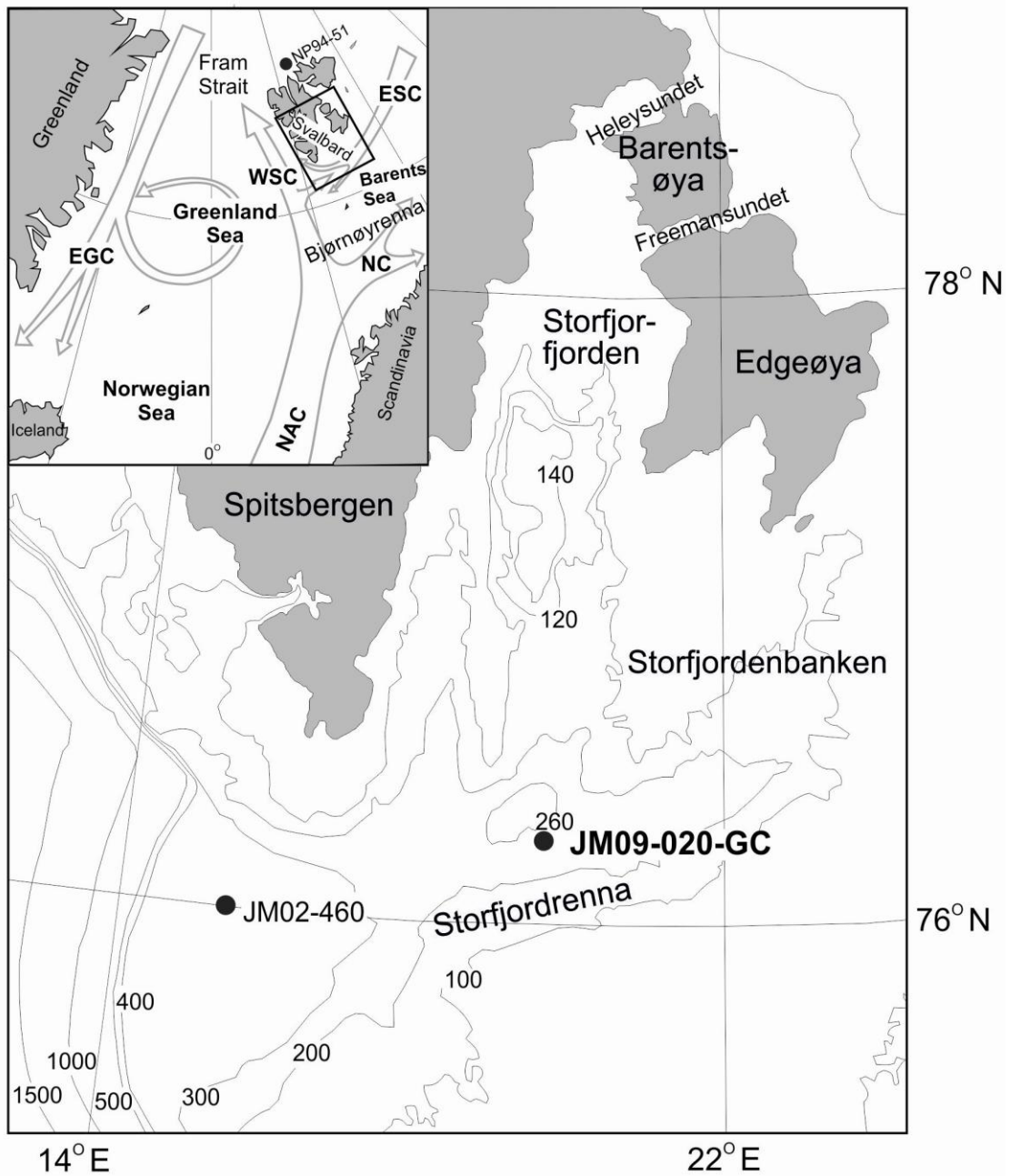
1132

1133

1134

1135

1136

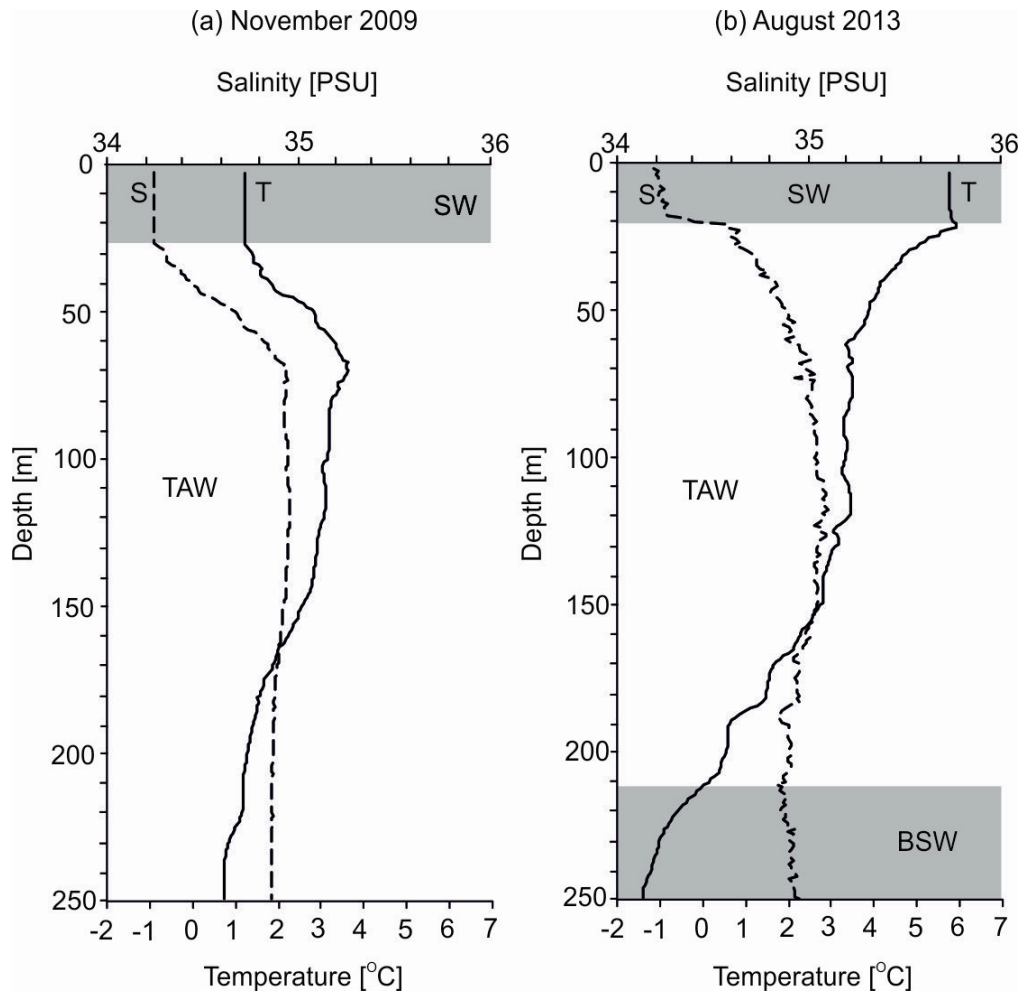


1138  
1139

1140

1141 Fig. 1. Location map (a) showing the core site from this study (JM09-020-GC) and core site  
1142 of JM02-460 (Rasmussen et al., 2007). The inset map (b) shows the modern surface oceanic  
1143 circulation in Nordic Seas and location of a core NP94-51 (Ślubowska et al., 2005).  
1144 Abbreviations: NAC- Norwegian-Atlantic Current; WSC- West Spitsbergen Current; ESC-  
1145 East Spitsbergen Current; EGC- East Greenland Current; NC- Norwegian Current. The cores  
1146 JM02-460 and NP94-51 are discussed in the text.

1147



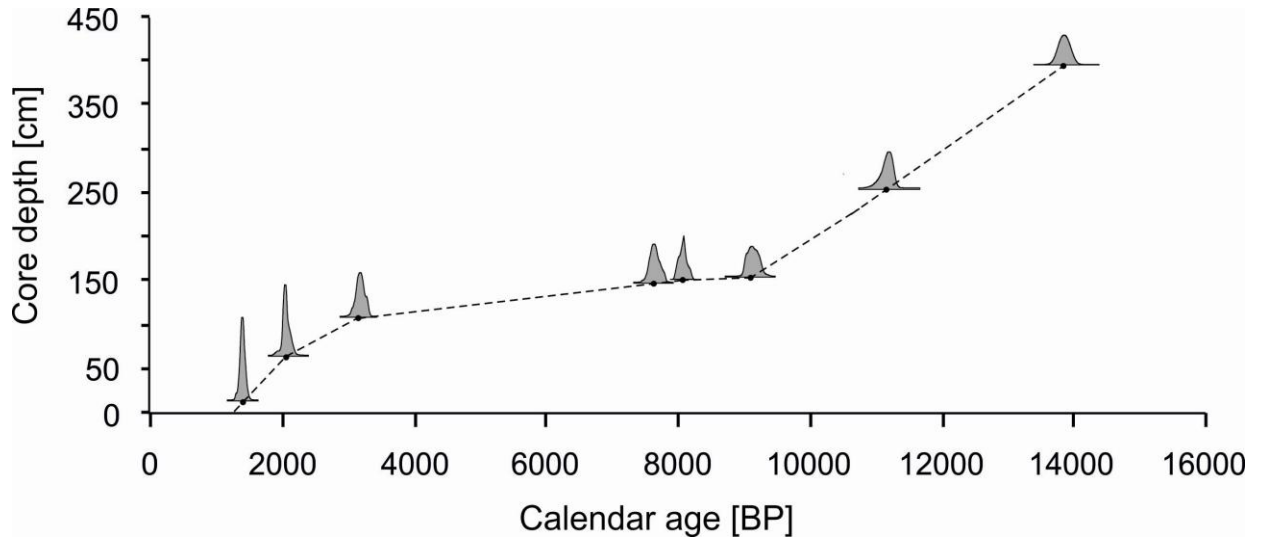
1148

1149

1150 Fig. 2. Temperature and salinity versus depth, measured in November 5<sup>th</sup> 2009 (a) and in  
 1151 August 13<sup>th</sup> 2013 (b) at the site of core JM09-020GC. SW - Surface Water, TAW -  
 1152 Transformed Atlantic Water, BSW - Brine-enriched Shelf Water.

1153

1154

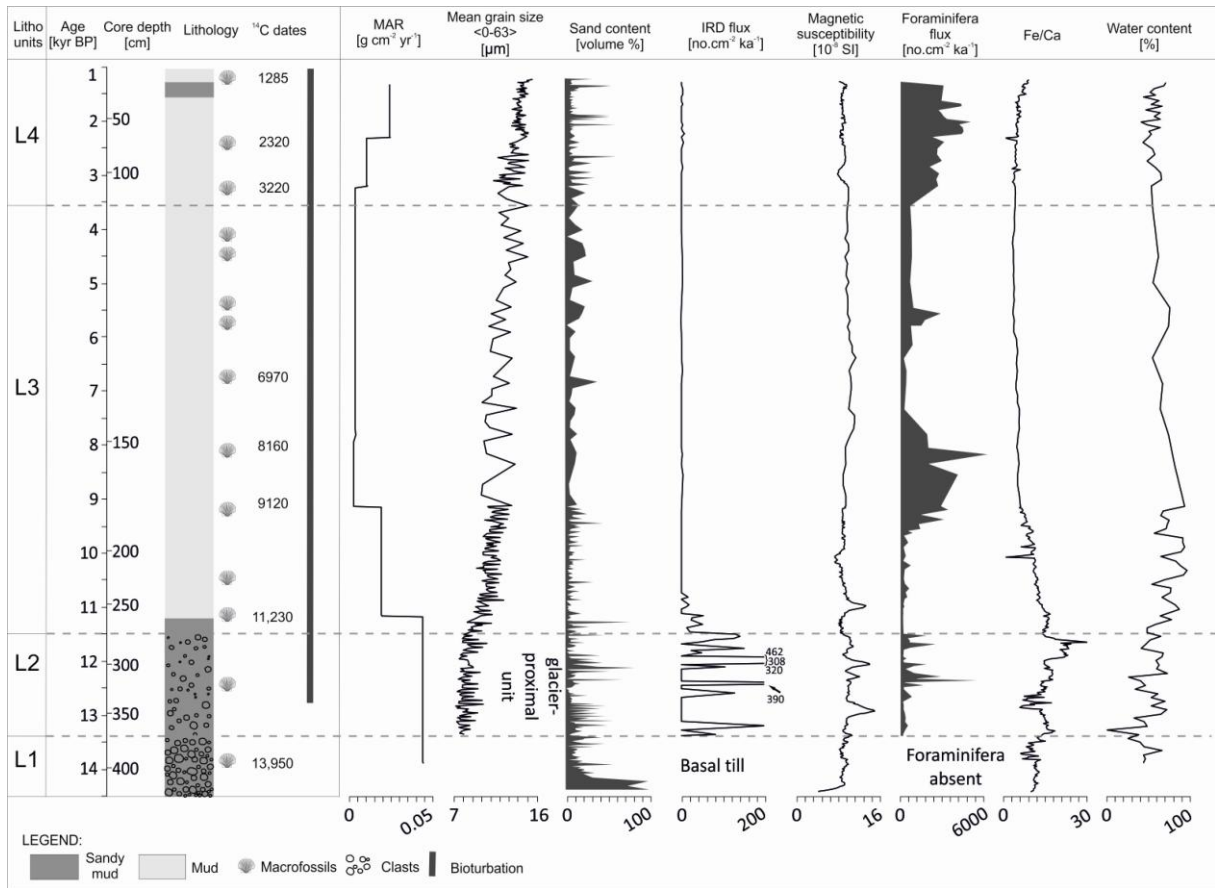


1155  
1156

1157 Fig. 3. Age-depth relationship for JM09-020-GC based on 8 AMS  $^{14}\text{C}$  calibrated ages with 2-  
1158 sigma age probability distribution curves. The chronology is established by linear  
1159 interpolation between the calibrated ages.

1160  
1161  
1162  
1163  
1164

1165

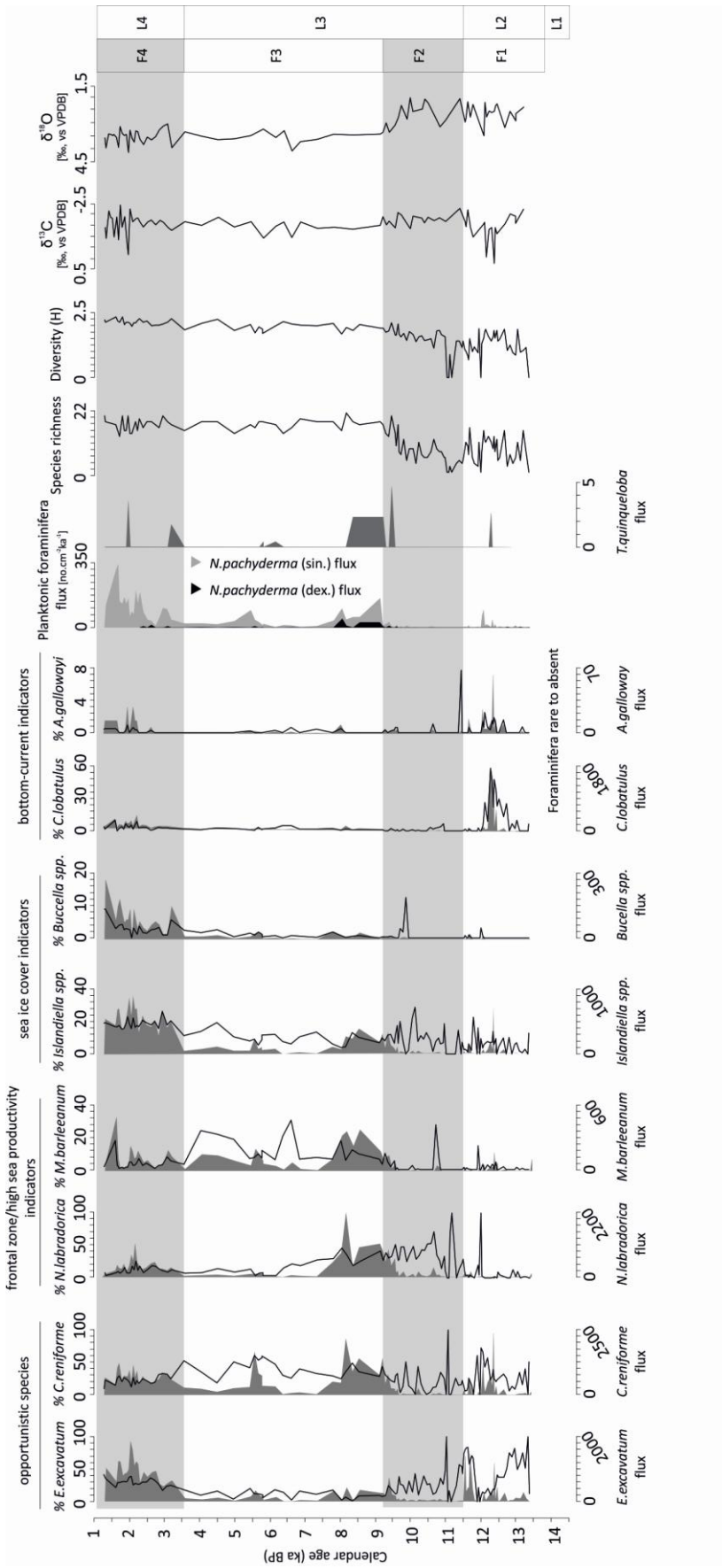


1166  
1167

1168

1169 Fig. 4. Lithological log of core JM09-020GC. Lithology, <sup>14</sup>C dates, occurrence of  
 1170 bioturbation, mass-accumulation rates, mean grain size in the range of 0-63 μm, sand content,  
 1171 ice-rafted debris flux, magnetic susceptibility, foraminifera flux as well as Fe/Ca ratio and  
 1172 water content. The results are presented with lithostratigraphic units (L1-L4), versus calendar  
 1173 years (cal kyr BP) and core depth (cm).

1174





1176 Fig. 5. Percentage distributions (upper scale; black line) of the most dominant benthic species,  
1177 fluxes (no. cm<sup>-2</sup> ka<sup>-1</sup>; bottom scale; grey shading) of benthic and planktonic foraminiferal  
1178 species, diversity parameters (species richness and Shannon - Wiener index) and stable  
1179 oxygen and carbon isotope data ( $\delta^{18}\text{O}$  and  $\delta^{13}\text{C}$ ) plotted versus thousands of calendar years  
1180 with indicated foraminiferal zonation (zones F1-F4) and lithostratigraphic units (L1-L4).  
1181 Foraminiferal taxa are grouped based on their ecological tolerances described in the text.

1182

1183

1184

1185

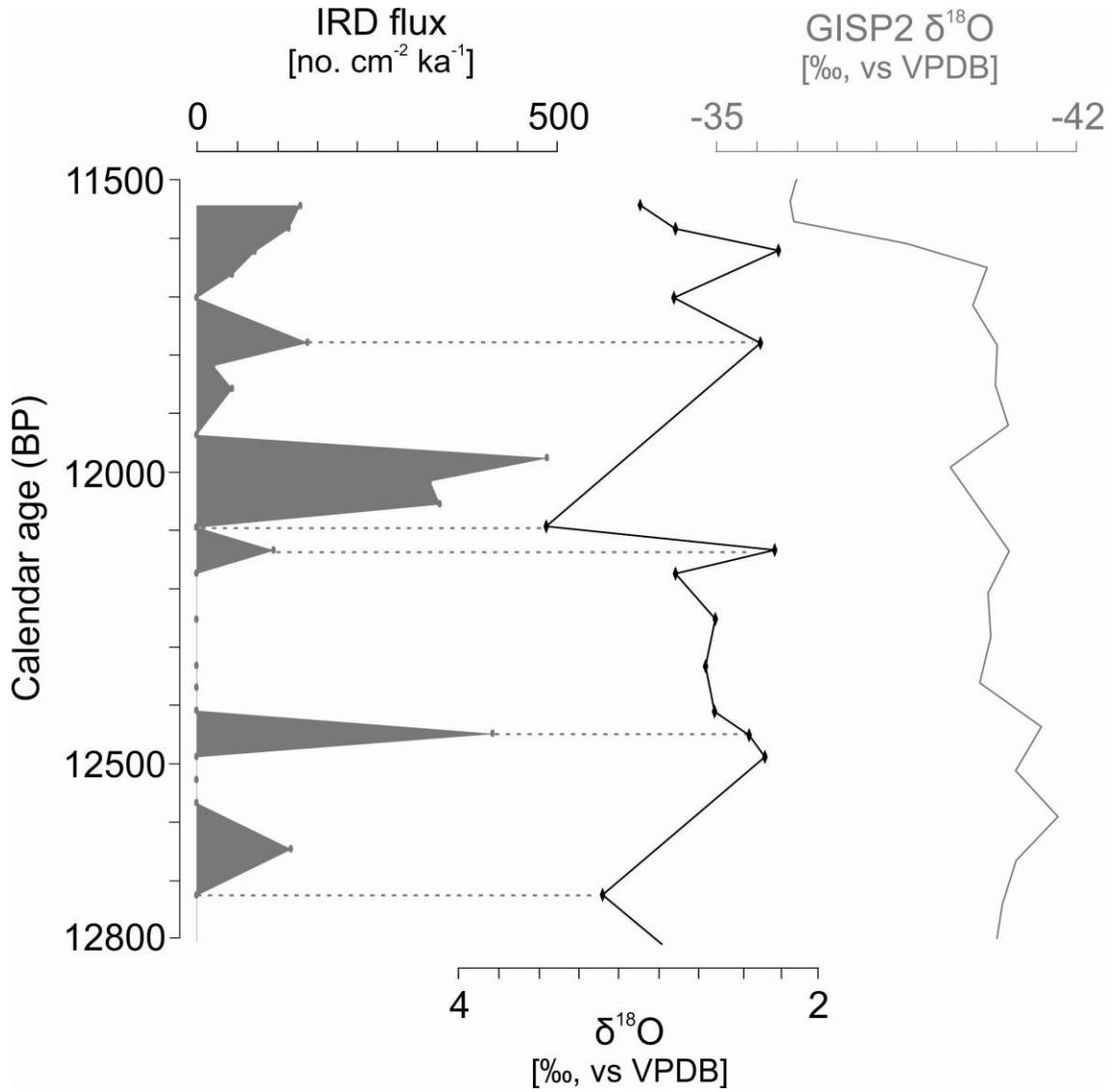
1186

1187

1188

1189

1190



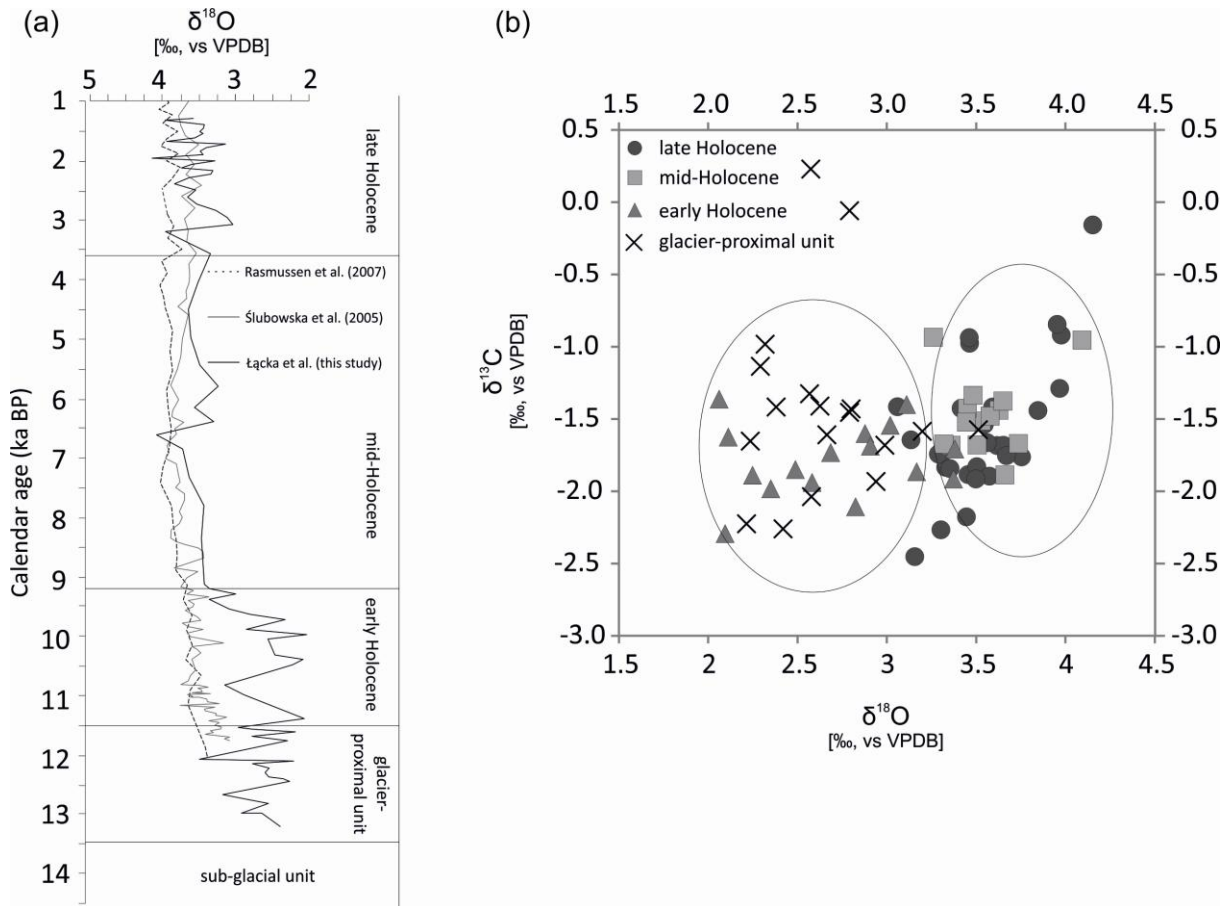
1191

1192

1193 Fig. 6 IRD flux (upper scale, grey shading) and oxygen stable isotopes records (bottom scale,  
 1194 black line) compared with oxygen stable isotopes records from ice core GISP2 from  
 1195 Greenland during the Younger Dryas period (12,800 cal yr BP to 11,500 cal yr BP).

1196

1197



1198  
1199

1200 Fig. 7 (a) The comparison of  $\delta^{18}\text{O}$  records (corrected for ice volume changes) between Łačka  
1201 et al. (this study; black solid line) and Ślubowska et al. (2005; grey solid line) and Rasmussen  
1202 et al. (2007; black dashed line) plotted versus thousands of calendar years. The  $\delta^{18}\text{O}$  records  
1203 after Łačka et al. (this study) were measured on *E.excavatum* f. *clavata* and the two latter ones  
1204 (Ślubowska et al., 2005 and Rasmussen et al., 2007) were measured on *M.barleeanum*. (b)  
1205 Scatter plot showing  $\delta^{13}\text{C}$  versus  $\delta^{18}\text{O}$  values from core JM09-020-GC (this study).

1206

1207